

Deep Learning–Accelerated Multi-Start Large Neighborhood Search for Real-time Freight Bundling

Haohui Zhang¹, Wouter van Heeswijk¹, Xinyu Hu¹, Neil Yorke-Smith², and Martijn Mes¹

¹*Department of High-Tech Business and Entrepreneurship, University of Twente, Enschede, Netherlands*

²*STAR Lab, Delft University of Technology, Delft, Netherlands*

December 15, 2025

Abstract

Online Freight Exchange Systems (OFEX) play a crucial role in modern freight logistics by facilitating real-time matching between shippers and carrier. However, efficient combinatorial bundling of transportation jobs remains a bottleneck. We model the OFEX combinatorial bundling problem as a multi-commodity one-to-one pickup-and-delivery selective traveling salesperson problem (m1-PDSTSP), which optimizes revenue-driven freight bundling under capacity, precedence, and route-length constraints. The key challenge is to couple combinatorial bundle selection with pickup-and-delivery routing under sub-second latency. We propose a learning–accelerated hybrid search pipeline that pairs a Transformer Neural Network-based constructive policy with an innovative Multi-Start Large Neighborhood Search (MSLNS) metaheuristic within a rolling-horizon scheme in which the platform repeatedly freezes the current marketplace into a static snapshot and solves it under a short time budget. This pairing leverages the low-latency, high-quality inference of the learning-based constructor alongside the robustness of improvement search; the multi-start design and plausible seeds help LNS to explore the solution space more efficiently. Across benchmarks, our method outperforms state-of-the-art neural combinatorial optimization and metaheuristic baselines in solution quality with comparable time, achieving an optimality gap of less than 2% in total revenue relative to the best available exact baseline method. To our knowledge, this is the first work to establish that a Deep Neural Network-based constructor can reliably provide high-quality seeds for (multi-start) improvement heuristics, with applicability beyond the *m1-PDSTSP* to a broad class of selective traveling salesperson problems and pickup and delivery problems.

1 Introduction

Trucking is the backbone of freight transportation in many countries. In recent years, Online Freight Exchange Systems (OFEX) platforms (e.g., Trans.eu and Uturn in Europe; Full Truck Alliance in China; Convoy, Coyote Logistics and Uber Freight in the United States) have become a common marketplace for shippers and carriers to connect and arrange services (Fazi and Fransoo 2025). These digital platforms facilitate seamless freight matching, real-time monitoring, and payment processing between shippers and carriers. By lowering search and transaction costs, these platforms assist in shippers reducing transport expenses and enable carriers, especially small operators, to find profitable backhauls, thereby reducing empty kilometers and improving market efficiency.

Beyond functioning as digital marketplaces, OFEX platforms have compelling economic incentives to integrate sophisticated algorithms to automate freight matching and optimize load allocation by analyzing comprehensive market data, carrier capacities, and demand patterns. By bundling shipments and recommending route-level assignments, these platforms can enable carriers to assemble feasible, profitable bundles of loads, thereby increasing revenue, equipment utilization, and ultimately driving a more efficient and profitable freight ecosystem.

Designing freight bundling algorithms for OFEX platforms remains understudied and highly challenging. OFEX markets are computationally centralized yet informationally decentralized: key information (e.g., future commitments) is private; loads and availability arrive asynchronously; and each shipment is exclusive (awarded to at most one carrier in each lane). In practice, platforms must recommend real-time backhaul and add-on bundles to many independent carriers under streaming arrivals and exclusivity, creating conflicts when similar bundles are provided to multiple carriers. Consequently, bundling couples combinatorial selection with pickup-and-delivery routing (an NP-hard problem even in static settings) while platforms operate under sub-second latency constraints that preclude exact methods during live allocation. This calls for low-latency bundling algorithms that jointly enforce pickup-and-delivery feasibility, equipment compatibility, and carrier-level preferences within a rolling horizon.

We model the OFEX combinatorial bundling problem as a multi-commodity one-to-one pickup-and-delivery selective traveling salesperson problem (*m1-PDSTSP*), a selective variant of the pickup-and-delivery traveling salesperson problem (PDTSP) in which each request has exactly one pickup node and one delivery node; requests are heterogeneous in size and value; and a single vehicle serves only a subset of requests subject to capacity and route-length constraints. The objective is to maximize revenue over all feasible pickup-and-delivery completions.

To meet real-time constraints, we adopt a rolling-horizon snapshot approach: although the market evolves continuously, the platform repeatedly solves static instances for a timescale shorter than market changes. To deliver high-quality bundles rapidly, we propose a learning-accelerated hybrid search algorithmic pipeline that combines the strengths of learning-based constructive heuristics

with the robustness of improvement heuristics. Specifically, we develop the deep learning (DL)-accelerated Multi-Start Large Neighborhood Search (MSLNS) for the $m1$ -PDSTSP, which leverages the Transformer neural network (Vaswani et al. 2017) and an innovative multi-start improvement heuristics. The Transformer-based policy scores and assembles requests into a feasible route-level bundle, producing plausible seed solutions rapidly that already respect pickup-and-delivery precedence, capacity, and route-length limits. These seeds are then refined by MSLNS, which provides diversification (multi-start + softmax-biased removal + adaptive destroy sizes) and intensification (improve with feasibility checks) to escape local optima and reduce the remaining optimality gap. To formalize the construction phase, we model the Transformer decoding process as a deterministic Markov Decision Process (MDP).

We elucidate the algorithmic rationale behind the hybrid pipeline and the design of MSLNS by analyzing attraction basins in neighborhood-based search, demonstrating how high-quality initializations and multi-start strategies accelerate convergence to superior local optima. Classical metaheuristics typically rely on random or greedy constructions to generate initial solutions, which often correspond to low-quality attractors located far from basins of superior local optima. As a result, substantial exploration (often requiring large neighborhood search) is needed, leading to higher computational cost and poor performance under tight latency constraints, as faced in the $m1$ -PDSTSP. By contrast, our neural constructor is empirically shown to rapidly produce high-quality seeds that position the search close to promising basins, enabling efficient improvement.

On benchmark instances, our approach outperforms state-of-the-art (SOTA) learning-based constructive heuristics and metaheuristics in solution quality and runtime: (i) Deep Neural Network (DNN)-generated solutions alone surpass metaheuristics initialized with greedy constructions while using less wall-clock time; (ii) appending a lightweight LNS improver to the DNN output outperforms learning-based constructive baselines that employ sophisticated search with less computational time; and (iii) the full DNN+MSLNS procedure achieves the lowest optimality gap in the majority of benchmark settings, under comparable wall-clock time. These results demonstrate the effectiveness of proposed hybrid pipeline, its practical potential for real-time routing, and the nontrivial role of high-quality initial solutions in improvement heuristics.

Contribution. (i) Conceptual: we formulate the $m1$ -PDSTSP to capture OFEX bundling and apply an attraction basin perspective to explain how initialization quality and multi-start strategies shape neighborhood-search performance. (ii) Methodological: We design an approximate feasibility-masking and reward-shaping scheme that enables efficient training of a Transformer-based policy-gradient constructor. Building on the insights from basin structure, we propose MSLNS, a multi-start large-neighborhood search procedure with softmax-biased removal and adaptive destroy sizes that exploits information embedded in learned trajectories to balance diversification and intensification.

(iii) Empirical: Through extensive computational experiments on *m1-PDSTSP* benchmarks, we demonstrate that our DL-accelerated MSLNS achieves superior performance against SOTA baselines. To the best of our knowledge, this is the first systematic demonstration that a neural constructor can reliably deliver high-quality initial solutions that measurably enhance (multi-start) improvement heuristics.

The remainder of the article is organized as follows. Sec. 2 reviews related work. Sec. 3 defines the *m1-PDSTSP*. Sec. 4 describes our methodology, including the motivation of learning-seeded hybrid search and the details of the proposed DL-accelerated MSLNS. Sec. 5 reports computational results and ablations. Sec. 6 concludes with a summary and directions for future research.

2 Related Work

We review related work on pickup and delivery problems (PDPs) and related solution approaches.

2.1 Pickup and Delivery Problems

Following Berbeglia et al. (2007), PDPs can be classified by the demand-supply structure into: (i) one-to-many-to-one (1-M-1), where all deliveries originate at the depot and all pickups return to the depot—also known as the TSP with pickup and delivery (TSPPD) defined by Mosheiov (1994); (ii) many-to-many (M-M), in which a single commodity is transported from supply to demand customers, yielding the one-commodity PDTSP (1-PDTSP) defined by Hernández-Pérez and Salazar-González (2003); and (iii) one-to-one (1-1), where each pickup is paired with exactly one delivery, underpinning the multi-commodity one-to-one PDTSP (m1-PDTSP) defined by Hernández-Pérez and Salazar-González (2009). The m1-PDTSP seeks a depot-to-depot tour that executes all paired pickups and deliveries under vehicle-capacity limits while minimizing travel distance.

In this study, we catalog the single-vehicle PDP formulations according to the attributes of demand-supply structure, node, vehicle, customer and commodity following Ting and Liao (2013). Tab. 1 summarizes representative variants and highlights their differences. Demand-supply structure includes 1-1, 1-M-1, and M-M. Node attributes cover selectivity (optional visits), depot supply/demand (whether the depot dispatches loads or receives them), and multiple visits (revisits allowed). Vehicle attributes include capacity bounds and route-length/time-window limits. Customer attributes include time windows and service type (pickup, delivery, or both). Finally, commodity attributes distinguish homogeneous (single-type) from heterogeneous (multi-type) requests.

The proposed *m1-PDSTSP* is a 1-1 pickup-and-delivery variant with heterogeneous requests and selectivity under capacity and route-length constraints, and each node requires either a pickup or a delivery. Tab. 1 situates *m1-PDSTSP* relative to prior PDP/TSP variants along these axes.

Table 1: Comparison between single vehicle PDP variants and the $m1$ -PDSTSP. (*Sel*: selectivity, *Dep*: depot supply/demand, *Vis*: multiple visits, *Ser*: service, *TW*: time window, *Cap*: capacity. *p*: pickup only, *d*: delivery only, $p\&d$: pickup and delivery at a visit, $p\&/d$: only pickup or only delivery or both at a visit, *HO*: homogeneous, *HE*: heterogeneous.) We list only one exemplary paper per problem due to space constraints.

Problem	Scheme	Node			Vehicle		Customer		Commodity	Reference
		Sel	Dep	Vis	Cap	TW	TW	Ser		
STSP	-	✓			✓				-	Laporte and Martello (1990)
PCTSP	-	✓			✓				-	Balas (1989)
TSP	-	✓							-	Feillet et al. (2005)
SP	M-M				✓			$p\&/d$	<i>HE</i>	Anily and Hassin (1992)
SPDP	M-M	✓			✓			p,d	<i>HO</i>	Ting and Liao (2013)
CTSPDP	M-M				✓			p,d	<i>HO</i>	Anily and Bramel (1999)
k-DeliveryTSP	M-M	✓			✓			p,d	<i>HO</i>	Chalasan and Motwani (1999)
1-PDTSP	M-M				✓			p,d	<i>HO</i>	Hernández-Pérez and Salazar-González (2003)
SD1PDTSP	M-M				✓			p,d	<i>HO</i>	Salazar-González and Santos-Hernández (2015)
1-TSP-SELDP	M-M	✓			✓			p,d	<i>HO</i>	Falcom et al. (2010)
TSPB	1-M-1				✓			p,d	<i>HE</i>	Anily and Mosheiov (1994)
SVRPPD	1-M-1				✓			$p\&/d$	<i>HE</i>	Gribkovskaia et al. (2007)
SVRPPDSP	1-M-1	✓			✓			$p\&/d$	<i>HO</i>	Gribkovskaia et al. (2008)
TSPPD	1-M-1				✓			$p\&/d$	<i>HO</i>	Mosheiov (1994)
TSPPD	1-1							p,d	<i>HE</i>	Dumitrescu et al. (2010)
TSPPDF	1-1							p,d	<i>HE</i>	Erdogan et al. (2009)
TSPPDL	1-1							p,d	<i>HE</i>	Cordeau et al. (2010)
S-DARP	1-1				✓		✓	p,d	<i>HE</i>	Psarafis (1980)
S-PDPTW	1-1				✓		✓	p,d	<i>HE</i>	Van der Bruggen et al. (1993)
PDTSP	1-1				✓			p,d	<i>HE</i>	Kalantari et al. (1985)
PDTSPH	1-1							p,d	<i>HE</i>	Veenstra et al. (2017)
PDTSPN	1-1							p,d	<i>HE</i>	Gao et al. (2023)
m-PDTSP	1-1				✓			$p\&/d$	<i>HO</i>	Hernández-Pérez and Salazar-González (2014)
m1-PDTSP	1-1				✓			$p\&/d$	<i>HE</i>	Hernández-Pérez and Salazar-González (2009)
m1-PDSTSP	1-1	✓			✓	✓		p,d	<i>HE</i>	This article

Algorithmically, these attributes reshape both the search space and the feasibility geometry: selectivity couples subset choice with routing; 1-1 structure imposes paired, path-dependent constraints; heterogeneous requests break exchangeability; and tight capacity and route-length restriction create near-infeasible faces (i.e., boundary regions of the feasible set) where naïve local edits (e.g., a simple swap) fail. Consequently, effective solution approaches must be feasibility-aware (e.g., paired destroy-repair, masking) and budget-conscious to operate in real time.

2.2 Solution Approaches

Heuristic algorithms trade off optimality guarantees for speed and scalability when solving a combination optimization problem (COP). They employ problem-specific hard-coded rules or general search strategies to quickly construct high-quality solutions when exact or provably-approximate methods are impractical due to large search spaces or tight time budgets. The aim is to deliver a feasible, effective solution within a reasonable timeframe, even if the result is suboptimal.

Generally, heuristics are functionally categorized into constructive and improvement heuristics (Kassoumeh et al. 2025). We refer to them as constructors and improvers, respectively. Constructors start with an empty solution and iteratively build a complete one by adding elements according to a specific construction rule (often a greedy strategy) selecting the best available element at each step. While efficient and fast, such approaches may be trapped in local optima

due to their myopic nature. By contrast, improvers begin with an existing solution and iteratively refine it by exploring its neighborhood. By systematically modifying the current solution, they can escape poor initial configurations and often achieve higher-quality results for a complex combinatorial optimization problems, but with more computational effort compared with constructors.

A large body of research on improvers focuses on effective neighborhood exploration by employing mechanisms such as acceptance ratios in Simulated Annealing (SA), tabu lists in Tabu Search, and nosing and randomization strategies in Adaptive Large Neighborhood Search (ALNS) to achieve proper diversification (Pisinger and Ropke 2018). While a few studies quantify the effect of the initial solution (e.g., Liu et al. 2024, Kassoumeh et al. 2025), most empirical studies detail operators and stopping conditions, yet keep the initializer fixed or omit it entirely, leaving its impact underexplored, especially under tight computational budgets where search trajectories are short. Typically, improvers obtain their initial solutions from either random generation or greedy constructors. Both methods can rapidly produce complete, feasible solutions from scratch, but they do not consistently provide high-quality solutions across diverse instances due to their greedy nature and lack of global perspective. This limitation motivates learning-based constructors that leverage learned representations of the problem structure to rapidly generate plausible starts for improvers.

2.2.1 Learning-based Heuristics

Neural Combinatorial Optimization (NCO) solvers or data-driven optimization leverage machine learning techniques to solve COPs. These methods typically involve training DNNs to learn stochastic policies (an end-to-end pretrained model) that can generate approximate solutions efficiently. The crux of learning-based heuristics is their capability to generalize from training data, allowing them to adapt to new problem instances without the need for extensive manual tuning. Following Wu et al. (2024), NCO methods are classified into Learning-to-Construct (L2C), Learning-to-Improve (L2I), and Learning-to-Predict (L2P).

L2C methods (e.g., Vinyals et al. 2015, Kool et al. 2018), including the SOTA Policy Optimization with Multiple Optima (Kwon et al. 2020) with diverse rollouts and data augmentation, build solutions sequentially by selecting the next unvisited node to extend a partial tour. L2I methods (e.g., Chen and Tian 2019, Ma et al. 2021) mimic iterative ruin-and-repair to refine incumbents. L2P approaches (e.g., Xin et al. 2021, Sun and Yang 2023) predict routing-related features such as structure signals or heatmaps that guide classical optimization algorithms during search. In practice, L2C typically offers the fastest inference but may require long training and can struggle to escape local optima; L2I explores richer neighborhoods but can stall in vast, complex search spaces; and L2P may generalize poorly when instance sizes or constraint regimes shift (Wu et al. 2024). Moreover, L2I/L2P are commonly trained with imitation/supervised signals distilled from high-quality heuristics or exact solvers, making near-optimal labels costly (or infeasible at scale) for new problem variants. This challenge is amplified in selective routing, where the solver must

jointly decide which customers to serve and how to route them under operational constraints. By contrast, L2C methods naturally accommodate selectivity: (i) they are commonly trained with reinforcement learning (RL), avoiding reliance on teacher labels; (ii) they can be shaped to construct profit-maximizing routes under constraints by masking infeasible actions; and (iii) they can provide more robust cross-regime generalization under moderate shifts in instance size and constraint tightness by learning global ordering/selection priors (e.g., long-range pickup-delivery compatibility) rather than teacher-specific labels. Accordingly, we adopt L2C as the backbone of our hybrid pipeline.

Existing neural-based methods predominantly address unselective routing problems, particularly specializing on well-studied instances such as the TSP and vehicle routing problem (VRP). Conversely, effective NCO methods for PDPs and selective problems remain under-explored. For PDPs, Li et al. (2021) introduce a heterogeneous attention model (heter-AM) trained with REINFORCE and a greedy rollout baseline proposed by Kool et al. (2018), effectively capturing precedence and outperforming simple heuristics and neural baselines on PDTSP; Ma et al. (2022) propose Neural Neighborhood Search (N2S) with a synthesis-attention decoder and tailored remove-reinsert operators to handle precedence, achieving competitive results versus LKH3 on canonical PDP variants; Kong et al. (2024) develop Neural Collaborative Search (NCS), a hybrid that couples neural construction and improvement via curriculum and imitation learning under a shared-critic scheme, outperforming standalone neural methods. Heter-AM is a L2C approach, but its added complexity yields little benefit over the attention model of Kool et al. (2018). The N2S and NCS methods are L2I approaches, relying on a heavy Transformer architecture and costly training. No prior work integrates feasibility masking with a Transformer under a selective PDP setting and none utilizes DL-generated solutions as informed seeds to guide improvement heuristics.

2.2.2 Large Neighborhood Search

LNS, introduced by Shaw (1998), is a powerful improvement metaheuristic that iteratively destroys and repairs parts of a solution to escape local optima. Starting from an initial solution, each iteration selects one destroy and one repair operator: the destroy phase randomly removes a small subset of customers, and the repair phase reinserts them to improve the objective under feasibility constraints. Originally developed for the VRP with time windows, LNS has been adapted to the PDP with time windows (PDPTW) (Bent and Van Hentenryck 2006). Building on this idea, Ropke and Pisinger (2006) propose ALNS, which maintains multiple destroy/repair operators and adaptively selects among them based on observed performance, achieving promising results on PDPTW variants (e.g., Masson et al. 2013, Ghilas et al. 2016). Operator scores are updated over time, biasing the selection toward higher-performing pairs as the search progresses. Unlike standard ALNS/LNS, which destroys requests uniformly, randomly, or by ad hoc scores, our MSLNS uses frequency signals from multiple neural trajectories to identify backbone requests and bias removal accordingly.

Coupled with an increasing destroy-size schedule, this creates a learning-driven diversification–intensification mechanism that standard LNS frameworks do not provide. Moreover, prior LNS work largely targets visit-all VRP/PDP settings, whereas selectivity fundamentally changes basin geometry and neighborhood structure, making our integration of neural guidance and selective routing genuinely new.

3 Problem Formulation

We formulate the OFEX combinatorial bundling problem as a *m1-PDSTSP*. Each request has exactly one pickup vertex and one delivery vertex, a demand, and a revenue. A capacitated vehicle departs from an origin and finishes at a destination within a route-length limit. The vehicle may serve only a subset of requests satisfying pickup-before-delivery precedence and capacity feasibility along the route. Equivalently, this is a capacitated selective TSP with precedence and paired-demand constraints. The problem is NP-hard by reduction from Hamiltonian path problem. We now present the formal model (the Mixed Integer Linear Programming formulation is in the Appendix 7.1).

3.1 Mathematical Formulation

Let $\mathcal{G} = (\mathcal{V}, \mathcal{E})$ be a complete undirected graph, where $\mathcal{V} = \mathcal{P} \cup \mathcal{D} \cup \{0, 2n+1\}$ consists of pickup vertices $\mathcal{P} = \{1, \dots, n\}$, delivery vertices $\mathcal{D} = \{n+1, \dots, 2n\}$, a start vertex 0, and an end vertex $2n+1$. Here n is the selected number of requests from the marketplace. For each request $h \in \mathcal{H} := \{1, \dots, n\}$, pickup $i_h \in \mathcal{P}$ is paired with delivery $i_h+n \in \mathcal{D}$ (pickup-before-delivery precedence). Each request has demand $q_h \in \mathbb{N}$ and revenue $r_h \in \mathbb{R}_{\geq 0}$, collected only if the request is delivered. For each edge $(i, j) \in \mathcal{E}$, the travel cost (distance) c_{ij} satisfies the triangle inequality ($c_{ij} \leq c_{ik} + c_{kj}$ for all i, j, k); edges represent shortest distances between locations.

We consider one vehicle with capacity Q and a maximum route-length T , starting at 0 and ending at $2n+1$. A feasible solution consists of (i) a subset of served requests $\Pi \subseteq \mathcal{V}$ and (ii) a permutation π of Π specifying the sequence of the vertices on the depot-to-depot route. We define that a route $\pi = \{0 = v_1, v_2, \dots, v_\tau = 2n+1\}$ is feasible if (i) the vehicle stops at most once in each vertex, (ii) the load capacity on the vehicle never exceeds the vehicle’s maximum capacity Q , (iii) the total length of the route does not exceed the pre-specified bound T : $c(\pi) \leq T$, where $c(\pi) = \sum_{i=1}^{\tau-1} c_{v_i, v_{i+1}}$, and (iv) if a pickup vertex is visited, then its delivery vertex must be visited afterwards (not necessarily immediately after). An example is provided in Fig. 1 with $n = 5$ requests, $Q = 5$, $T = 15$ and a feasible route $\pi = (0, 4, 3, 2, 7, 5, 9, 8, 10, 11)$ with final route-length 13.3 and collected revenue 9.

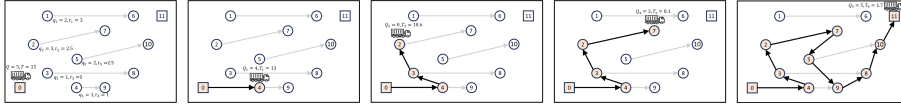


Figure 1: Example of the $m1$ -PDSTSP with $n = 5$ requests and a feasible solution $\pi = (0, 4, 3, 2, 7, 5, 9, 8, 10, 11)$.

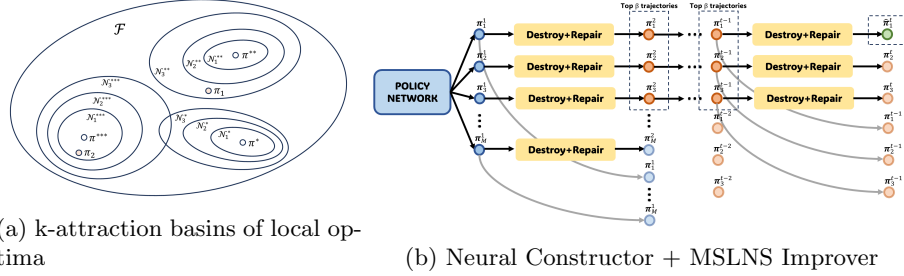
4 Solution Methodology

To effectively address the $m1$ -PDSTSP, we propose a learning-seeded hybrid search pipeline in Fig. 2 that combines a deep learning constructor with powerful improvement heuristics. This pipeline has two phases: the constructor generates high-quality initial solutions rapidly; after which the improver refines these solutions to approach local optima. This synergy leverages the strengths of both components, yielding superior performance on complex routing problems.

In this section, we first elaborate the conceptual motivation behind this design (Sec. 4.1). We then formulate the algorithmic procedure of the constructor as a MDP (Sec. 4.2) and detail its DNN architecture with an approximate feasibility masking scheme (Sec. 4.3), and training (POMO; Sec. 4.3.3). Finally, we describe the improvement heuristic, namely the MSLNS (Sec. 4.4).

4.1 Conceptual Motivation

Given an instance, a local optimal solution is an *attractor* if it is a fixed point of the local search operator (i.e., greedy insertion repair Alg. 5 in Appendix 8). An *attraction basin* is the subset of the search space from which the local search dynamics converge to the same attractor (Jerebic et al. 2021). We define $\mathcal{N}_k(\pi)$ as the set of solutions in the k -neighborhood of a solution π , i.e., solutions that can be reached from π by applying a destroy-repair operator that removes k requests and reinserts them. Within $\mathcal{N}_k(\pi)$, for any π and $k \geq 1$, multiple attractors may exist. A solution π^* is called a k -*attractor* (with respect to \mathcal{N}_k) if $f(\pi^*) \geq f(\pi)$ for all $\pi \in \mathcal{N}_k(\pi^*)$; the corresponding $\mathcal{N}_k(\pi^*)$ is referred to as the k -*attractor basin*. Because the $m1$ -PDSTSP is selective, attraction basins are determined by the served-request set. Reaching an *attractor* is relatively easy, whereas reaching a superior k -*attractor* is substantially more challenging. The Best-improvement LNS (BI-LNS) improver (Appendix 8.1) with k -destroy operator is guaranteed to converge to the k -*attractor* as it exhaustively explores the associated k -*attractor basin* of the initial solution. If the initial solution lies near a high-quality basin (e.g., π_2 in Fig. 2a), convergence to the global optimum π^{***} (where $f(\pi^{***}) = \max_{\pi} f(\pi)$) can be achieved with relatively small k . Conversely, starting from a distant solution (e.g., π_1) significantly hampers success even for SOTA metaheuristics, particularly for LNS variants that explore only a portion of the basin. Starting from multiple diverse and high-quality initial solutions can mitigate this issue by probing multiple high-quality basins in parallel.



(a) k -attraction basins of local optima

(b) Neural Constructor + MSLNS Improver

Figure 2: In the left figure, π^* , π^{**} are local optima, π^{***} is the global optimum ($f(\pi^*) \leq f(\pi^{**}) \leq f(\pi^{***})$) and \mathcal{N}_k are their related k -attraction basins. From initial solutions π_1 and π_2 , BI-LNS readily reach π^{***} from π_2 , whereas π_1 lies far from the high-quality basins and struggles to reach even π^{**} . In the right figure, the policy network (Transformer) generates multiple initial solutions in parallel and iteratively refines them with MSLNS to obtain the final solutions (keeping a fixed-width β candidates).

Although the solutions produced by the DNN are not guaranteed to be globally optimal or even attractors themselves (see Sec. 5), they tend to fall within the attraction region of high-quality basins more often than those generated by classical constructors. Consequently, they provide high-quality initializations that guide downstream improvers with small k toward superior local optima (see Fig. 4 in Appendix 9), explaining the consistent effectiveness of our hybrid pipeline.

4.2 Markov Decision Process for Route Construction

As the constructors construct the solution auto-regressively, the generation process is inherently sequential (Drakulic et al. 2023). This mirrors the structure of a sequential decision-making problem, where decisions influence both future feasibility and attainable reward. Modeling the decoding procedure as a MDP makes this dependence explicit and provides a principled framework for defining (partial routes), actions (selectable requests), transition rules (updating feasibility), and rewards (incremental revenue). This formulation clarifies what the neural policy is learning, why masking matters, and where the main computational challenges arise under selective PDP constraints.

Formally, we denote a COP instance by $\min_{x \in \mathcal{F}} f(x)$, where \mathcal{F} is the (finite) set of feasible, complete solutions, and $f : \mathcal{F} \rightarrow \mathbb{R}$ is the objective (e.g., negative collected revenue). Equivalently, feasibility can be encoded by a global constraint predicate $C(\cdot)$ with $\mathcal{F} = \{x : C(x) = \text{T}\}$.

Given a solution space $(\mathcal{X}, \circ, \epsilon, \mathcal{Z})$, where \mathcal{X} denotes the set of all possible and feasible partial solutions for a given COP, \mathcal{Z} denotes the set of elementary construction steps (adding one pickup vertex, one delivery vertex or the end vertex z^e), \circ is the concatenation operator and ϵ is the neutral element (formal

definition is in Appendix 7.4), we consider the set $\mathcal{S}_{\mathcal{X}}$ of instances (f, \mathcal{F}) . The MDP resulting denoted by $\mathcal{M}_{(f, \mathcal{F})}$ is defined as follows:

State space: $\bar{\mathcal{X}} := \{x \in \mathcal{X} : \exists y \in \mathcal{Z}^* \text{ with } x \circ y \circ z^e \in \mathcal{F}\}$, i.e., partial solutions that can be extended (by a finite sequence of steps from \mathcal{Z}) to some feasible complete solution in \mathcal{F} .

Action space: $\mathcal{A} := \{z \in \mathcal{Z} : C(x \circ z) = \mathbb{T}\} \cup \{\epsilon\}$, which is state dependent, i.e., an action is either a step (adding an unvisited vertex) or the neutral action ϵ .

Deterministic transition: The transition function is deterministic, and can be represented as a labelled transition system with the following two rules, with actions serving as transition labels:

$$x \xrightarrow[f(x)-f(x \circ z)]{z} x \circ z \text{ if } x \circ z \in \bar{\mathcal{X}} \quad , \quad x \xrightarrow[0]{\epsilon} x \text{ if } x \in \mathcal{F}. \quad (1)$$

Here $x \in \bar{\mathcal{X}}$ is a state and $z \in \mathcal{Z}$ is a step.

Reward function: $r(x, z) = f(x) - f(x')$ where $x, x' \in \bar{\mathcal{X}}$, and $x' = x \circ z$ for all $z \in \mathcal{Z}$ or $x' = x$ when $z = \epsilon$. Starting from $x_0 = \epsilon$, an episode applies admissible actions until reaching a terminal state $x_\tau \in \mathcal{F}$. Because we *minimize* f , maximizing the cumulative return $\sum_{t=1}^{\tau} r(x_t, a_t) = f(x_0) - f(x_\tau)$ is equivalent to driving $f(x_\tau)$ as low as possible.

To minimize the objective function f of the *m1-PDSTSP* defined in (11), the stochastic policy p_θ automatically selects a vertex at each time step based on a learned distribution under the operational constraints. This process is repeated iteratively until the policy chooses to visit the end vertex. The policy produces a sequence of the selected vertices that specifies the vehicle’s visit order, $\pi = (z_1 \circ z_2 \circ \dots \circ z_\tau)$, where z_1 and z_τ are the start and end vertices of the vehicle, respectively. Based on the chain rule, the probability of an output solution is factorized as follows,

$$p_\theta(\pi | s) = \prod_{t=1}^{\tau} p_\theta(z_t | \mathbf{z}_{1:t-1}, s), \quad \forall s \in \mathcal{S}_{\mathcal{X}}. \quad (2)$$

4.2.1 MDP-Transformer Integration

In Fig. 3, we couple the MDP with the Transformer by formalizing the state at time t as $\tilde{x}_t = (\mathbf{h}, \bar{\mathbf{h}}, x_t)$, where \mathbf{h} and $\bar{\mathbf{h}}$ are the node embeddings and the global instance embedding learned by the encoder (which are shared across all time steps, see details in Sec. 4.3.1), and $x_t = \mathbf{z}_{1:t-1}$ is the partial solution maintained up to time t . The action z_t , generated by the decoder, is the next feasible vertex to visit. The reward $r_t = f(x_{t-1}) - f(x_t)$ captures the one-step improvement in the objective. An episode terminates when the policy

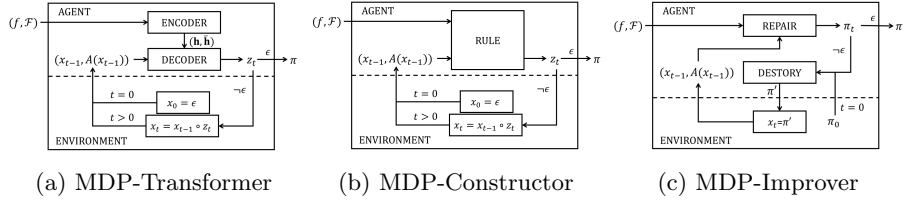


Figure 3: Illustrations of MDP integrating with a Transformer, a constructor and an improver (Appendix 7.5).

selects the end vertex, i.e., $z_\tau = z^\epsilon$. The total return is thus $R = \sum_{t=1}^{\tau} r_t = f(\epsilon) - f(z_{1:\tau}) = -f(\pi)$. As for the constructive metaheuristics, the state at time t is x_t and the policy is rule-based (i.e., fitness).

4.2.2 Computational Challenges

In the constructive process, evaluating the action space at each step requires validating the feasibility of adding each unvisited vertex to the current partial solution, formally, for each $z \in \mathcal{Z}$, validating whether $C(x \circ z) = \text{T}$. This is computationally expensive because even validating a single capacity-feasible pickup involves verifying that its paired delivery, all yet-undelivered vertices, and the end vertex can still be visited within route-length limits, an NP-hard, shortest-Hamiltonian-path problem (see Fig. 7, fourth panel; requests 3 and 4 remain undelivered, and validating whether picking up request 1 or 3 is admissible requires such a test). Because this validation may be performed for every candidate action at every construction step, it effectively embeds an NP-hard subproblem inside the inner loop, causing the computational cost to scale combinatorially with the number of undelivered vertices and unvisited pickup vertices. Repeatedly solving such validations during the training of the neural networks is intractable without aggressive approximation or pruning. To accelerate this, we propose an approximate feasibility masking scheme (in Sec. 4.3.2) that screens candidates based on cheap lower bound surrogates. This validation also happens in repair operator, which motivates an efficient searching algorithm.

4.3 Details of Attention Model

To enable the hybrid pipeline, we require a neural constructor capable of producing strong, feasibility-aware initial solutions. Accordingly, our attention model builds on Kool et al. (2018) and Kwon et al. (2020); we customize both the encoder-decoder Transformer architecture and the policy-gradient training procedure for the *m1-PDSTSP*.

4.3.1 Encoder

The encoder maps instance features into contextualized embeddings via self-attention, producing keys/values for the decoder to score feasible actions.

Node feature embeddings: From the $d_{\mathbf{x}}$ -dimensional input features \mathbf{x}_i , the encoder computes initial $d_{\mathbf{h}}$ -dimensional node embeddings $\mathbf{h}_i^{(0)}$ ($d_{\mathbf{h}} = 128$) via a learned type-specific linear map:

$$\mathbf{h}_i^{(0)} = \begin{cases} W_{\text{depot}}^{\mathbf{x}} \begin{bmatrix} \mathbf{y}_i, T \end{bmatrix} + \mathbf{b}_{\text{depot}}^{\mathbf{x}} & i = 0, 2n + 1 \\ W_{\text{pickup}}^{\mathbf{x}} \begin{bmatrix} \mathbf{y}_i, \mathbf{y}_{i+n}, \hat{q}_i, \hat{r}_i \end{bmatrix} + \mathbf{b}_{\text{pickup}}^{\mathbf{x}} & i = 1, \dots, n \\ W_{\text{delivery}}^{\mathbf{x}} \begin{bmatrix} \mathbf{y}_i, -\hat{q}_i, \hat{r}_i \end{bmatrix} + \mathbf{b}_{\text{delivery}}^{\mathbf{x}} & i = n + 1, \dots, 2n, \end{cases} \quad (3)$$

The input features include the node coordinates $\mathbf{y}_i \in \mathbb{R}^2$, normalized demand $\hat{q}_i \in [0, 1]$ if i is a pickup node and $-\hat{q}_i$ if i is a delivery node, and normalized revenue $\hat{r}_i \in [0, 1]$ (normalization ensures that all inputs share a comparable scale).

Afterwards, the node embeddings go through L attention layers, each of which encompasses a multi-head attention (MHA) sublayer ($M = 8$ heads with dimensionality $d_{\mathbf{h}}/M = 16$) and a feed-forward (FF) sublayer (one hidden layer with dimension 512 and ReLU activation). We denote with $\mathbf{h}_i^{(\ell)}$ the node embeddings produced by layer $\ell \in \{1, \dots, L\}$. Similar to Kool et al. (2018), each sublayer adds a skip-connection and batch normalization (BN):

$$\hat{\mathbf{h}}_i = \text{BN}^{\ell} \left(\mathbf{h}_i^{(\ell-1)} + \text{MHA}_i^{\ell} \left(\mathbf{h}_0^{(\ell-1)}, \dots, \mathbf{h}_{2n+1}^{(\ell-1)} \right) \right), \quad \mathbf{h}_i^{(\ell)} = \text{BN} \left(\hat{\mathbf{h}}_i + \text{FF}^{\ell}(\hat{\mathbf{h}}_i) \right). \quad (4)$$

Graph embedding: The encoder computes an aggregated embedding $\bar{\mathbf{h}}^{(L)}$ of the input instance as the mean of the node embeddings at the final layer $\bar{\mathbf{h}}^{(L)} = \frac{1}{2n+2} \sum_{i=1}^{2n} \mathbf{h}_i^{(L)}$.

4.3.2 Decoder

The decoding is auto-regressive and happens sequentially. At timestep $t \in \{1, \dots, 2n + 1\}$, the decoder generates a probability for selecting a node z_t based on the embeddings $(\mathbf{h}_i^{(\ell)}, \mathbf{h}_i^{(\ell)})$ from the encoder and the outputs $\mathbf{z}_{1:t-1}$ generated before time t .

Operational Constraints: To facilitate the capacity and maximum length constraints, we keep track of the remaining normalized capacity \hat{Q}_t and remaining length T_t at time t . At $t = 1$, $\hat{Q}_1 = 1$ and $T_1 = T$, thereafter, they are updated as follows:

$$\hat{Q}_{t+1} = \max(\hat{Q}_t - \hat{q}_{z_t}, 0), \quad T_{t+1} = T_t - c_{z_{t-1}, z_t}, \quad (5)$$

where c_{z_{t-1}, z_t} is the distance from node z_{t-1} to z_t and we define $z_0 = 0$.

Context Embedding: The context for the decoder for *m1-PDSTSP* at time t includes the node embeddings of the current location z_{t-1} and the end location of the vehicle $2n+1$, the remaining capacity \hat{Q}_t , and the remaining route length T_t : $\mathbf{h}_{(c)}^{(L)} = [\bar{\mathbf{h}}^{(L)}, \mathbf{h}_{z_{t-1}}^{(L)}, \mathbf{h}_{2n+1}^{(L)}, \hat{Q}_t, T_t]$, where $[\cdot, \cdot]$ is the horizontal concatenation operator. We compute a new context node embedding $\mathbf{h}_{(c)}^{(L+1)}$ using the MHA mechanism (described in Appendix 7), where the context embedding serves as the query. The keys and values are derived from the node embedding $\mathbf{h}_i^{(L)}$, allowing the context to aggregate relevant information from all nodes through attention ($\mathbf{q}_{(c)}^{(L)} = W^Q \mathbf{h}_{(c)}^{(L)}$, $\mathbf{k}_i = W^K \mathbf{h}_i^{(L)}$, $\mathbf{v}_i = W^V \mathbf{h}_i^{(L)}$).

Masking: During decoding, all invalid nodes are dynamically masked at each step to ensure solution feasibility. Upon departing from the start node, all delivery nodes are initially masked. If there are undelivered deliveries, the end node is masked. After visiting a pickup node, its corresponding delivery node is unmasked, while all visited nodes (incl. the start node) are masked. Pickup nodes are also masked if their demand exceeds the current remaining capacity. Finally, each unvisited pickup node j is masked if serving j , completing all yet-undelivered deliveries, and reaching the end node would violate the remaining route-length limit. In principle, validating this last condition requires, at each step and for each unvisited pickup node, solving a shortest Hamiltonian path problem, an NP-hard problem that is prohibitively expensive to perform millions of times during training. We therefore design a lower-bound screening: for each pickup node j , we compute a cheap lower bound surrogate on the route length using only the current node j , its delivery node $j+n$, and the end depot $2n+1$; if this surrogate already exceeds the remaining time limit, j is masked. This avoids the hard feasibility validation and reduces the per-candidate test from $\mathcal{O}(n^2)$ by 2-Opt (which provides an approximation of the minimum route length) to $\mathcal{O}(1)$. The trade-off is that some infeasible pickup nodes may not be masked and be selected by the policy.

We denote the resulting potential cost of visiting a pickup node j at step t by \tilde{c}_j as follows:

$$\tilde{c}_j = \begin{cases} c_{z_{t-1},j} + c_{j,j+n} + c_{j+n,2n+1} & \text{if training,} \\ c_{z_{t-1},j} + \text{TwoOpt}_{j,2n+1}(S) & \text{if inference,} \end{cases} \quad (6)$$

where $\text{TwoOpt}_{s,t}(S)$ returns the tour obtained by applying 2-Opt to a path constrained to start at s and end at t while visiting all nodes in S ; here $S \subseteq \{n+1, \dots, 2n\}$ denotes all yet-undelivered delivery nodes including $j+n$. Initialized from a nearest-neighbor tour, 2-Opt typically removes detours and substantially shortens the route. We apply it as an more accurate validator, executed in parallel across the batch. Given that the lower bound may be loose, some infeasible nodes may remain unmasked, we shape the reward (objective) function to penalize infeasible solutions:

$$\tilde{f}(\pi) = f(\pi) + \rho \cdot \max\{0, c(\pi) - T\}, \quad (7)$$

where ρ is a penalty coefficient and $c(\pi)$ is the total distance/length of the route π .

We compute the compatibility of the query with all nodes based on (28) in Appendix 7, and mask nodes which are not feasible. We define the mask matrix \mathcal{M}_t at time t for all $j \in V$ as follows:

$$\mathcal{M}_t[j] = \begin{cases} -\infty & \text{if } \exists t' < t : \pi_{t'} = j \text{ or } \nexists t' < t : \pi_{t'} = \max\{0, j - n\} \text{ or } \hat{q}_{j,t} > \hat{Q}_t \text{ or } \tilde{c}_j > T_t, \\ 1 & \text{otherwise.} \end{cases} \quad (8)$$

Finally, we add one final single attention head decoder layer to compute the probability vector p_θ . The next node is sampled from the p_θ using the categorical distribution during training:

$$p_i = p_\theta(z_t = i | s, \mathbf{z}_{1:t-1}) = \text{softmax}\left(C \cdot \tanh\left(\frac{\mathbf{q}_{(c)}^{(L+1)\top} \mathbf{k}_j}{\sqrt{d_k}} \odot \mathcal{M}_t\right)\right), \quad (9)$$

where $C = 10$, $d_k = \frac{d_h}{M}$ is the query and key dimensionality, and \odot denotes the Hadamard (element-wise) product. This process iteratively continues until the end node is visited.

4.3.3 Training Algorithm

During training, the problem instances are independently and identically distributed from a distribution \mathbb{S} . We adopt the SOTA training algorithm, Policy Optimization with Multiple Optima (POMO) (Kwon et al. 2020), to train multiple greedy trajectories. Our motivation differs from the original paper: POMO was designed for unselective, sequence invariant problems (e.g., TSP), where a symmetry-aware policy should produce the same solution regardless of the start node, and its optimizer exploits this symmetry. In our selective setting, solutions are not sequence invariant. The starting action significantly affects feasibility and quality, as a poor start can accumulate deviations throughout decoding. We therefore leverage POMO’s multi-start strategy to emphasize start-node selection and broaden exploration over the solution space.

POMO begins with the vehicle start node and selects M different pickup nodes $\{z_1^1, z_1^2, \dots, z_1^M\}$ to start for exploration, where $z_1^j \in \mathcal{P}$, $j \in \{1, \dots, M\}$, and $M \leq |\mathcal{P}|$. The M start pickup nodes are the top M choices of the stochastic policy p_θ given by the current policy network. As our problem is selective and anchored at a fixed start node, the full POMO multi-start over all nodes is unnecessary. Accordingly, we restrict POMO to $M = n/2$ parallel starting positions (one per pickup) rather than $|V|$. Then the network samples M solution trajectories $\{\pi^1, \pi^2, \dots, \pi^M\}$ via Monte-Carlo simulation by drawing B i.i.d. sample instances $s_1, \dots, s_B \sim \mathbb{S}$. Based on (34) in Appendix 7.3, in POMO, we apply the shared baseline (to reduce variance and stabilize training) for all $j \in M$ and $i \in B$:

$$b^j(s_i) = b_{\text{shared}}(s_i) = \frac{1}{M} \sum_{k=1}^M \tilde{f}(\pi_i^k). \quad (10)$$

The training procedure is summarized in Alg. 1.

Algorithm 1 Policy Optimization with Multiple Optima (POMO) Training

```

1: Input: number of epochs  $E$ , steps per epoch  $K$ , batch size  $B$ , number of start nodes  $M$ 
2: Initialize policy parameters  $\theta$ 
3: for epoch = 1, ...,  $E$  do ▷ outer training loop
4:   for step = 1, ...,  $K$  do ▷ mini-batch updates per epoch
5:      $s_i \leftarrow \text{RANDOMINSTANCE}() \quad \forall i \in \{1, \dots, B\}$  ▷ sample a batch of instances
6:      $\{\pi_{1,i}^1, \pi_{1,i}^2, \dots, \pi_{1,i}^M\} \leftarrow \text{SELECTSTARTPICKUPNODES}(s_i) \quad \forall i \in \{1, \dots, B\}$  ▷  $M$  diverse starts per instance
7:      $\pi_i^j \leftarrow \text{SAMPLEROLLOUT}(\pi_{1,i}^j, s_i, p_\theta) \quad \forall i \in \{1, \dots, B\}, \forall j \in \{1, \dots, M\}$  ▷ roll out a full solution from each start
8:      $b_i \leftarrow \frac{1}{M} \sum_{j=1}^M \tilde{f}(\pi_i^j) \quad \forall i \in \{1, \dots, B\}$  ▷ per-instance baseline: mean objective over  $M$  starts
9:      $\nabla \mathcal{L} \leftarrow \frac{1}{BM} \sum_{i=1}^B \sum_{j=1}^M (\tilde{f}(\pi_i^j) - b_i) \nabla_\theta \log p_\theta(\pi_i^j)$  ▷ REINFORCE gradient with baseline
10:     $\theta \leftarrow \text{ADAM}(\theta, \nabla \mathcal{L})$  ▷ optimizer update

```

4.4 Multi-Start Large Neighborhood Search

To apply a multi-start strategy, a straightforward way is to run LNS independently on each trajectory; however, this is computationally inefficient and fails to exploit the structural information provided by the DNN. Because the neural constructor generates multiple greedy trajectories independently, the frequency with which a request appears across these trajectories reflects its relative importance (or lack of substitutability) within the instance. To leverage this information, we design a softmax-biased removal strategy that selects requests to destroy simultaneously across all trajectories. We prioritize high-frequency requests for early removal because they typically repair back into the solution, revealing backbone structure that can be fixed so that subsequent search concentrates on escaping low-quality basins rather than rediscovering stable route components. Moreover, the destroy size controls the search regime: small destroy sizes favor intensification within a basin, whereas larger sizes enable transitions across basins.

For illustration, consider 10 requests with a global optimum $\{0, 3, 5, 7, 9\}$ and a local 1-attractor $\{0, 1, 2, 3\}$. Destroying 1 first leads repair back to the same attractor, when each request is destroyed at most once (as in our experiments to ensure efficient exploration), the subsequent search can never reach the global optimum. By contrast, destroying 0 first allows transitions (e.g., via subsequent removals of $\{1, 2\}$, $\{2, 3\}$, or $\{1, 3\}$) that open paths to basins containing the global optimum.

Based on these insights, we design MSLNS with the following components: (i) destroy operator with softmax-biased removals and a short-term memory of deleted requests to avoid redundant deletions; (ii) an increasing destroy-size schedule; (iii) greedy insertion repair operator; and (iv) multi-start diversification. Specifically, the destroy step first deduplicates identical served-request sets across the candidates, then selects requests that have not yet been marked

Algorithm 2 Multi-Start Large Neighborhood Search (MSLNS)

Require: M initial trajectories Π , beam width β , reward function R , time limit t_{\max} , temperature α , max removals k_{\max}

- 1: $\mathcal{U} \leftarrow \emptyset$; $i \leftarrow 1$ ▷ Memory of removed requests
- 2: **while** time $< t_{\max}$ **do** ▷ Main search loop until time limit
- 3: $(\mathbf{u}, \mathbf{c}) \leftarrow \text{COUNTUNIQUE}(\Pi) \setminus \mathcal{U}$ ▷ Find unremoved unique requests and their counts
- 4: **if** $(\mathbf{u}, \mathbf{c}) = \emptyset$ **then break end if** ▷ Stop if no requests left to destroy
- 5: $\mathbf{p} \leftarrow \text{softmax}(\alpha \mathbf{c})$; $\mathbf{u}^* \sim \text{Multinomial}(\mathbf{p}, \min\{i + 1, k_{\max}\})$ ▷ Sample k requests to destroy based on weighted counts
- 6: $\mathcal{U} \leftarrow \mathcal{U} \cup \mathbf{u}^*$ ▷ Record destroyed requests in memory
- 7: $\Pi' \leftarrow \text{REPAIR}(\text{DESTROY}(\Pi, \mathbf{u}^*))$ ▷ Apply destroy-repair to generate new candidate trajectories
- 8: $\Pi' \leftarrow \text{TWOOPT}(\text{DEDUP}(\Pi'))$ ▷ Local improvement and duplicate removal
- 9: $\Pi \leftarrow \text{TOP}_{\beta}(\Pi \cup \Pi', R)$ ▷ Keep top- β solutions by reward
- 10: $i \leftarrow i + 1$ ▷ Increase removal budget for next iteration
- 11: **return** $\arg \max_{\pi \in \Pi} R(\pi)$

for destruction by sampling from a softmax over their frequencies across all trajectories (temperature $\alpha = 1$; larger α biases more toward frequent requests). We gradually increase the destroy size from 2 up to $k_{\max} = 4$. The repair step selects best-insertion greedily (Alg. 5 in Appendix 8). Because running LNS on all trajectories is costly, we adopt a pruning strategy that retains a fixed-width set of top β candidates at each iteration, and we further apply a fast 2-Opt pass to improve the travel distance for each candidate. The overall procedure appears in Fig. 2b and Alg. 2. In practice, MSLNS only destroys a request at most once because of the time budget and the high-quality initial solutions produced by the policy network. We choose POMO (M parallel greedy rollouts as Alg. 4 in Appendix 8) as the constructor due to its effectiveness in training and its natural ability to produce multiple high-quality, diverse greedy trajectories for MSLNS. Through extensive experiments in next section, we verify the robustness of MSLNS with different constructors and the effectiveness of each component in it.

5 Experiments

In this section, we investigate how initialization quality, attraction basin structure, and neighborhood design jointly determine search effectiveness in selective PDPs under tight latency constraints. Our empirical study has three goals: (i) characterize the strengths and limitations of classical heuristics, neural constructors, and hybrid methods; (ii) quantify the contribution of each MSLNS component; and (iii) assess robustness across instance scales and problem regimes. To this end, we evaluate our POMO+MSLNS approach on the *m1-PDSTSP* against the following neural baselines: AM (Kool et al. 2018), POMO (Kwon et al. 2020), and POMO-SGBS (Choo et al. 2022); heuristic baselines: GS, Hill Climbing (HC), Multi-Start Greedy Search (MSGS), BI-LNS, LNS, and SA; and Gurobi v12.0.3. All baselines are implemented and tuned for our setting in Appendix 8. Then, we conduct ablations to quantify the contributions of

individual MSLNS components. Additional analyses, including sensitivity to revenue parameters, route-length limits, and zero-shot generalization, are reported in Appendix 9. These results further demonstrate the robustness of the learning-seeded hybrid search design and the strong cross-regime generalization of POMO+MSLNS.

5.1 Experimental Setup

We detail instance generation, training protocol, and inference/time-budget settings.

Instance Generation: All instances are randomly generated. Following the settings in Li et al. (2021), the location of the depots and customer (pickup and delivery pair) nodes are randomly and independently drawn from a uniform distribution in the unit square $[0, 1]^2$. The traveling cost between two nodes are measured by Euclidean distance. The demand of each customer node is uniformly sampled from the set $\{2, 3, 4, 5\}$. For the distribution of the revenue, we consider four variants: *Distance*, *Ton-Distance*, *Uniform* and *Constant*. We normalize the revenue r_h such that $\hat{r}_h \in [0, 1]$ for all $h \in \mathcal{H}$. For the *Distance* setting, the revenue is proportional to the distance between the pickup and delivery nodes. This distance-based normalization mirrors distance-driven earnings/costs and keeps results comparable across instances (the details of latter three are in Appendix 9). We sample capacity $Q \sim \text{Unif}\{8, \dots, 20\}$ and set the route-length budget $T \sim \text{Unif}\{\max\{2, \lceil \frac{3n}{20} c_{0,2n+1} \rceil\}, \dots, \max\{2, \lceil \frac{10n}{20} c_{0,2n+1} \rceil\}\}$, anchoring T to the start-end depot distance $c_{0,2n+1}$ and scaling with instance size n . This enables Q commensurate with per-stop demands, enabling non-trivial consolidation without trivial full coverage, while the range of T yields time budgets from tight to relaxed, ensuring that capacity and route-length constraints frequently influence feasibility. Regarding the scale, the problem sizes are set to $N = \{22, 42, 82, 122\}$ (incl. two depots and all nodes of pickup and delivery), and are denoted by PDSTSP22/42/82/122.

Training: To compare AM and POMO fairly, we train both on the instances randomly generated from the same generator. AM follows Kool et al. (2018) with 2500 batches \times 512 instances per epoch; POMO employs 2000 batches \times 64 instances per epoch. Both share the same policy network (encoder depth $N = 3$) and apply the Adam with initial learning rate 10^{-4} (and weight decay 10^{-6} for POMO), without learning-rate decay. All runs execute on a single NVIDIA A100 GPU (120 GB memory). To compute them equally, we set the number of training epochs as in Tab. 2, so that each method receives approximately the same wall-clock time.

Inference: For each problem, we report performance on a test set of 1,000 instances generated with the same procedure as the training set but different random seeds. All experiments were run on CPU only, using a 32-vCPU machine, and we report the corresponding runtimes. For most algorithms, runtime

Table 2: Training hyperparameters

Instance	PDSTSP22	PDSTSP42	PDSTSP82	PDSTSP122
AM	150 epochs (20 min/epoch)	125 epochs (40 min/epoch)	150 epochs (80 min/epoch)	125 epochs (120 min/epoch)
POMO	200 epochs (15 min/epoch)	200 epochs (25 min/epoch)	200 epochs (60 min/epoch)	150 epochs (100 min/epoch)

and performance can be traded off by adjusting hyperparameters. Since reporting full trade-off curves is impractical, we instead select representative configurations that strike a reasonable balance between runtime and solution quality. The chosen hyperparameters are summarized in Tab. 4 in Appendix 8. Since larger instances make each repair more expensive, we scale the per-instance time limit t_{max} with instance size ($= 0.5s/1s/4s/10s$ for PDSTSP22/42/82/122).

5.2 Experimental Results

Our main experiments focus on the *Distance* setting, as it has the most practical significance. We define a metric Winning Rate (WR) to measure the percentage of instances where an algorithm achieves the best-known solution among all compared methods (including the exact Gurobi solver when available). WR captures how often a method attains top performance and also reflects how frequently its solutions fall within the 0-attraction basin of the best-known solution, complementing the optimality gap metric. A higher WR indicates more consistent excellence across instances. We can only attain the optimum for small instances using Gurobi within practical runtime.

Given Tab. 3, we observe: (i) among the heuristic baselines, $MSG+MSLNS_{[5,3]}^{t_{max}}$ ($M = 5, \beta = 3$, under t_{max} time limit) attains the best performance on all scales, highlighting the effectiveness of multi-start exploration even without learned guidance; (ii) neural methods significantly outperform classical heuristics with lower wall-clock time (especially at larger scales), underscoring their superior scalability; (iii) hybrid methods that combine neural constructors with LNS consistently outperform standalone neural methods (even with sophisticated search), which often fail to reach an *attractor* as even simple HC can further improve them; (iv) $POMO+MSLNS_{[10,5]}^{t_{max}}$ generally outperform all the other methods ($< 2\%$ gaps on total revenue and high WRs across all scales), demonstrating that high-quality neural initialization and structured multi-start neighborhood exploration are complementary; (v) $POMO+MSLNS_{[10,10]}$ nearly matches Gurobi on PDSTSP22 (gap=0.57% and WR=88.2%), confirming that $POMO+MSLNS$ can approach exact-solver quality; (vi) POMO variants outperform AM variants at larger scales, suggesting that POMO’s multi-start training yields more robust policies for large-scale selective routing; (vii) AM consistently achieve higher WR than GS, and neural methods equipped with sophisticated search attain higher WR than neighborhood search initialized from GS, indicating that neural constructors reach the 0-attraction basin of the best-known solution more frequently than classical constructors, thereby providing more reliable starting points for downstream improvement; (viii) $AM-BS+BI-LNS^{t_{max}}$ and $POMO-SGBS_{[5,5]}$ achieve high WR at all scales, suggesting that they ex-

Table 3: Performance matrix: PDSTSP22/42/82/122 on *Distance*.

Algorithm	PDSTSP22					PDSTSP42					PDSTSP82					PDSTSP122					
	Tim	Rev	Pro	Gap	WR	Tim	Rev	Pro	Gap	WR	Tim	Rev	Pro	Gap	WR	Tim	Rev	Pro	Gap	WR	
Heuristics	GS+2-Opt	10s	1.80	-0.55	18.76%	17.8%	2m	3.83	0.08	24.55%	3.0%	12m	7.93	1.48	28.79%	0.3%	50m	12.59	2.84	30.17%	0.0%
	GS+HC	17s	1.92	-0.53	13.19%	28.6%	3m	4.18	0.19	17.50%	6.8%	13m	8.66	1.64	22.19%	0.9%	53m	13.63	2.94	24.42%	0.0%
	GS+BNS ^{t_{max}}	8m	2.04	-0.46	8.74%	41.9%	12m	4.45	0.43	12.24%	11.6%	1.4h	9.14	2.10	17.86%	2.1%	3.6h	14.42	3.73	19.99%	0.6%
	GS+LNS ^{t_{max}}	82s	2.02	-0.47	7.91%	44.6%	18m	4.42	0.40	12.86%	11.8%	1.5h	9.09	2.05	18.31%	2.1%	3.5h	14.79	4.10	17.94%	0.7%
	GS+SA ^{t_{max}}	9m	2.14	-0.37	3.49%	70.0%	23m	4.38	0.37	13.65%	15.6%	1.6h	8.96	1.93	19.49%	3.3%	3.8h	14.18	3.50	21.31%	1.2%
	GS+SA						2.8h	4.70	0.68	7.25%	32.6%	3.3h	9.50	2.46	14.66%	7.6%	9.4h	14.88	4.19	17.43%	2.9%
	MSGs	53s	2.01	-0.48	9.51%	36.8%	11m	4.26	0.26	16.04%	7.3%	1.7h	8.81	2.26	20.91%	1.6%	6.7h	13.92	4.05	22.77%	0.1%
MSGs+MNS _[5,3] ^{t_{max}}	4m	2.17	-0.32	2.20%	74.9%	29m	4.73	0.73	6.80%	27.5%	3.1h	9.68	2.66	13.05%	6.2%	10.5h	15.25	4.58	15.40%	2.6%	
NCOs	POMO-single	6s	1.85	-0.57	16.76%	18.8%	49s	4.48	0.56	11.67%	4.6%	5m	10.10	3.18	9.27%	0.8%	11m	16.69	6.22	7.42%	0.1%
	AM	7s	1.97	-0.45	11.29%	28.7%	45s	4.54	0.62	10.49%	7.2%	5m	10.13	3.21	9.03%	1.1%	12m	16.52	6.02	8.34%	0.2%
	AM-sample	66s	2.03	-0.37	8.38%	35.8%	8m	4.74	0.79	6.53%	12.7%	1.7h	10.63	3.67	4.52%	4.0%	5.6h	17.34	6.83	3.80%	2.1%
	AM-MS	54s	2.10	-0.36	5.22%	47.5%	7m	4.79	0.83	5.53%	14.3%	1.7h	10.61	3.67	4.68%	4.9%	5.4h	17.24	6.74	4.38%	0.7%
	AM-BS	59s	2.13	-0.33	5.22%	55.7%	8m	4.82	0.86	4.90%	19.4%	1.7h	10.66	3.71	4.28%	6.0%	6.1h	17.27	6.77	4.20%	1.6%
	POMO	54s	2.08	-0.38	6.00%	43.8%	7m	4.79	0.83	5.50%	15.7%	1.7h	10.67	3.72	4.18%	4.4%	5.4h	17.44	6.95	3.26%	1.5%
	POMO-SGBS _[5,5]	3m	2.09	-0.40	5.88%	52.6%	40m	4.83	0.83	4.77%	23.5%	3.0h	10.82	3.84	2.77%	14.4%	9.8h	17.75	7.23	1.52%	19.5%
	AM-sample _[100]	11m	2.07	-0.37	6.48%	41.4%	1.3h	4.85	0.87	4.38%	16.4%										
	AM-BS _[100]	10m	2.13	-0.33	3.94%	56.5%	1.3h	4.88	0.91	4.38%	23.9%										
	Hybrids	AM+HC	23s	2.05	-0.40	7.69%	40.2%	2m	4.70	0.73	7.38%	14.3%	20m	10.44	3.47	6.22%	3.8%	1.3h	16.96	6.44	5.94%
AM+BNS ^{t_{max}}		87s	2.13	-0.37	4.00%	57.0%	11m	4.85	0.85	4.26%	28.8%	1.3h	10.65	3.64	4.34%	11.8%	4.4h	17.20	6.62	4.57%	8.1%
AM-BS+HC		75s	2.15	-0.31	3.02%	62.0%	9m	4.89	0.92	3.48%	28.2%	1.9h	10.83	3.87	2.73%	11.9%	7.2h	17.53	7.05	2.76%	5.1%
AM-BS+BNS ^{t_{max}}		2m	2.18	-0.31	1.83%	71.6%	17m	4.97	0.96	2.07%	41.1%	2.9h	10.93	3.92	1.83%	26.4%	10.3h	17.67	7.11	1.96%	17.9%
POMO+HC		71s	2.12	-0.34	4.26%	53.5%	10m	4.90	0.93	3.38%	27.1%	1.9h	10.86	3.90	2.43%	9.6%	6.6h	17.74	7.27	1.61%	4.5%
POMO+BNS ^{t_{max}}		2m	2.16	-0.34	2.80%	64.6%	17m	4.97	0.96	2.00%	40.1%	2.8h	10.98	3.98	1.40%	23.0%	9.8h	17.86	7.30	0.90%	20.7%
Ours	AM-MS+MNS _[5,3] ^{t_{max}}	5m	2.19	-0.30	1.19%	78.9%	25m	4.99	1.01	1.55%	44.0%	3.2h	10.93	3.97	1.84%	19.9%	10.0h	17.73	7.24	1.62%	12.5%
	POMO+MNS _[5,3] ^{t_{max}}	4m	2.19	-0.30	1.35%	78.1%	28m	4.99	1.00	1.65%	42.3%	3.1h	10.97	4.01	1.43%	18.7%	9.8h	17.86	7.38	0.91%	11.7%
	POMO+MNS _[10,5] ^{t_{max}}	7m	2.20	-0.30	0.96%	82.6%	40m	4.99	1.00	1.57%	43.2%	3.9h	10.99	4.03	1.24%	20.4%	12.4h	17.88	7.40	0.80%	12.4%
BLs	POMO+MNS _[10,10]	15m	2.20	-0.29	0.57%	88.2%	3.3h	5.07	1.08	0.00%	65.8%	12.7h	11.13	4.17	0.00%	48.5%	1.4d	18.03	7.54	0.00%	38.3%
	Gurobi (100s)	17.1h	2.22	-0.31	0.00%	97.7%															

BL: Baseline. Tim: Time, Rev: Revenue, Pro: Profit, Gap: Gap on Revenue. WR: Winning Rate. MNS: MSLNS, BNS:BI-LNS.

Profit (=Revenue-Length) is positively correlated with Revenue. Some LS run finish before the time budget due to early convergence, while some MSLNS exceed t_{max} when completing the final repair. Across all four scales, POMO+MSLNS_[10,5]^{t_{max}} generally achieves the best performance—among time-budgeted methods—but typically incurs higher runtime than other baselines.

plore attraction basins that are systematically different from those reached by MSLNS. While not achieving the lowest gap, they intermittently outperform by discovering instance-specific structures not captured by the latter.

Taken together, these results demonstrate that the hybrid pipelines dominates the quality-latency Pareto frontier (see Fig. 6 in Appendix 9) on the *m1-PDSTSP*. Practically, AM/AM+HC are plausible choices under tight budget, whereas POMO+BI-LNS and POMO+MSLNS should be the default for middle/high budget. The modest gains of MSLNS^{t_{max}} over BI-LNS^{t_{max}} arise because, for large T , MSLNS is less efficient and often cannot converge within the budget; hence, it can underperform BI-LNS (consistent with the evidence in Tab. 5 in Appendix 10.0.2).

Fig. 4 demonstrates that POMO+MSLNS consistently attains the highest fraction across all values of k on PDSTSP22, indicating that its solutions most frequently lie within the k -attraction basin of the best-known solution. In contrast, classical metaheuristics require substantially larger neighborhoods to reach the same basin. Among constructors, AM consistently outperforms HC

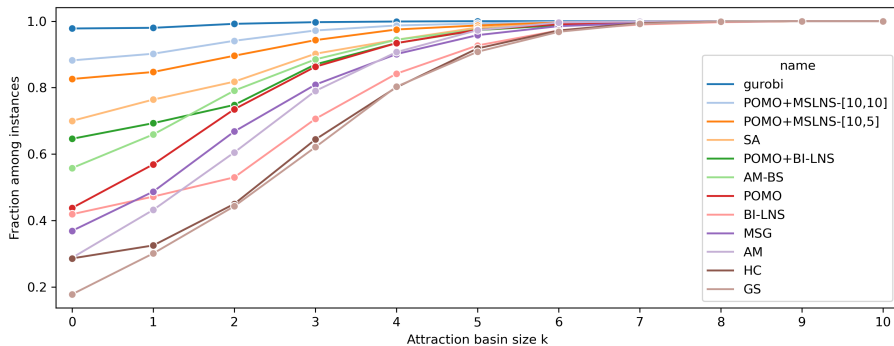


Figure 4: Fraction of solutions in the k -attraction basin of the best-known solution on PDSTSP22. Higher values at smaller k indicate closer proximity to high-quality attraction basins. Hybrid methods exhibit significantly stronger basin alignment than classical metaheuristics.

and GS, while POMO and AM-BS dominate MSG and BI-LNS across all k . Notably, MSG outperforms BI-LNS for small neighborhoods, highlighting the benefit of multi-start strategies. SA performs competitively in this setting due to the small instance size and relatively loose computational budget.

Overall, the results establish the necessity of the combination of a neural constructor and a heuristic improver to tackle the challenging $m1$ -PDSTSP, highlight the superior performance of POMO+MSLNS method, and underscore the importance of high-quality initialization and multi-start diversification for efficiently accessing high-quality attraction basins.

5.3 Ablation Study

In this section, we examine the importance of MSLNS components (softmax-biased removal, multi-start strategies, increasing destroy size) using a small set of 200 instances on *Distance* PDSTSP42. For a fair comparison, we fix the instance set and employ the same pretrained POMO for all variants. Each variant is run five independent times with different solver seeds to smooth out stochastic fluctuations from both the model and the search process. We report the mean.

MSLNS variants. (i) *Softmax+Inc-k (Full)*: softmax-biased removal, multi-start, increasing destroy size ($k_{max} = 4$); (ii) *Uniform+Inc-k*: replace softmax with uniform removal, keep increasing size ($k_{max} = 4$); (iii) *Softmax+Fixed-k*: softmax removal with fixed $k = 4$; (iv) *Uniform+Fixed-k*: uniform removal with fixed $k = 4$; (v) *Single-start*: set $M = 1$, others as in *Full*; (vi) *2-Opt+LNS*: apply a fast 2-Opt after the best solution given by POMO, then plain LNS with uniform removal with random $k \sim \text{Unif}\{1, 2, 3\}$, no multi-start. We also report: (i) *BI-LNS-only* and (ii) *2-Opt+BI-LNS*.

Fig. 5 presents that the full MSLNS (Softmax+Inc- k) achieves the best mean performance, both under time limits (mean=4.710) and at convergence

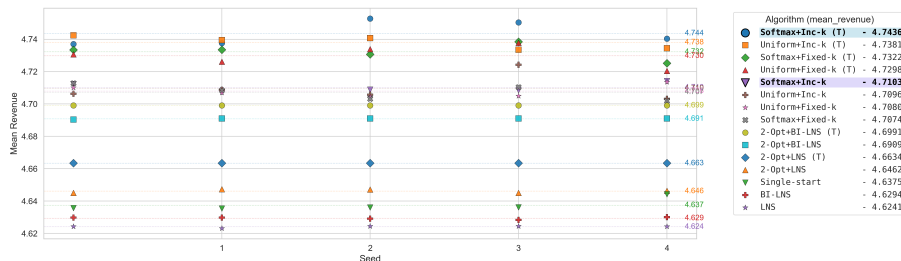


Figure 5: Ablation of MSLNS components on PDSTSP42 (*Distance*): mean revenue across all instances, running over five seeds. Methods marked “(T)” are unlimited-time variants (run to convergence). The unlimited full MSLNS—Softmax+Inc- k (T)—achieves the best performance.

(mean=4.744). Both components matter: fixing k or replacing softmax with uniform removal degrades quality, though limited-time variants narrow the gap slightly. Multi-start also helps: Single-start and 2-Opt+LNS drops notably (mean < 4.700). We further observe that a 2-Opt pass materially strengthens the LNS improver; BI-LNS-only (mean=4.629) underperforms relative to 2-Opt+BI-LNS (mean=4.691) across budgets. We note that the variance across five seeds is small, yielding stable behavior and consistent rankings. Overall, top performance requires the full configuration and dropping any component consistently lowers quality under both time-limited and converged runs.

6 Conclusion

We address real-time freight bundling on OFEX platforms by formulating the multi-commodity one-to-one pickup-and-delivery selective traveling salesperson problem (*m1-PDSTSP*), a selective problem that couples combinatorial bundle selection with pickup-and-delivery routing under tight latency constraints. Our algorithmic contribution is the learning-accelerated hybrid search pipeline, supported by attraction basin analysis and empirical evidence, that clarifies how neural construction, neighborhood-based improvement, and multi-start diversification can be effectively integrated for selective routing problems. We show that Transformer-based policy-gradient constructors can consistently generate solutions that lie within high-quality attraction basins, providing effective initializations for downstream neighborhood search. Building on this insight, we propose MSLNS, a multi-start metaheuristic with softmax-biased removal and adaptive destroy sizes, which systematically exploits basin structure to balance diversification and intensification. Extensive experiments demonstrate that this combination advances the quality-time frontier of selective PDP algorithms: compared to classical metaheuristics and standalone neural methods, the proposed hybrid pipeline closes optimality gaps more reliably under strict time budgets and approaches exact-solver performance on small instances while scaling effectively to larger ones. Beyond the specific *m1-PDSTSP*, the evidence

supports a broader algorithmic principle: high-quality learned initializations, when combined with basin-aware neighborhood exploration, can substantially enhance the effectiveness of improvement heuristics for selective TSP and PDP variants.

A key limitation is our reliance on rolling-horizon snapshots with fixed per-snapshot budgets: under bursty arrivals or very large instances, latency escalates and the method’s advantage over simpler heuristics diminishes, thereby limiting deployability at scale. Future work includes scaling our hybrid pipeline via hierarchical (e.g., region) decomposition and distributed LNS, enabling parallel search and preserving sub-second response time even on very large snapshots. We also plan to validate the algorithm on real-world OFEX instances with additional operational constraints (e.g., time windows), quantifying latency, stability, and improvements in utilization and revenue.

References

- Anily S, Bramel J (1999) Approximation algorithms for the capacitated traveling salesman problem with pickups and deliveries. *Naval Research Logistics (NRL)* 46(6):654–670.
- Anily S, Hassin R (1992) The swapping problem. *Networks* 22(4):419–433.
- Anily S, Mosheiov G (1994) The traveling salesman problem with delivery and backhauls. *Operations Research Letters* 16(1):11–18.
- Balas E (1989) The prize collecting traveling salesman problem. *Networks* 19(6):621–636.
- Bent R, Van Hentenryck P (2006) A two-stage hybrid algorithm for pickup and delivery vehicle routing problems with time windows. *Computers & Operations Research* 33(4):875–893.
- Berbeglia G, Cordeau JF, Gribkovskaia I, Laporte G (2007) Static pickup and delivery problems: a classification scheme and survey. *Top* 15:1–31.
- Chalasani P, Motwani R (1999) Approximating capacitated routing and delivery problems. *SIAM Journal on Computing* 28(6):2133–2149.
- Chen X, Tian Y (2019) Learning to perform local rewriting for combinatorial optimization. *Advances in neural information processing systems* 32.
- Choo J, Kwon YD, Kim J, Jae J, Hottung A, Tierney K, Gwon Y (2022) Simulation-guided beam search for neural combinatorial optimization. *Advances in Neural Information Processing Systems* 35:8760–8772.
- Cordeau JF, Iori M, Laporte G, Salazar González JJ (2010) A branch-and-cut algorithm for the pickup and delivery traveling salesman problem with lifo loading. *Networks* 55(1):46–59.
- Drakulic D, Michel S, Mai F, Sors A, Andreoli JM (2023) Bq-nco: Bisimulation quotienting for efficient neural combinatorial optimization. *Advances in Neural Information Processing Systems* 36:77416–77429.
- Dumitrescu I, Ropke S, Cordeau JF, Laporte G (2010) The traveling salesman problem with pickup and delivery: polyhedral results and a branch-and-cut algorithm. *Mathematical Programming* 121:269–305.

- Erdoğan G, Cordeau JF, Laporte G (2009) The pickup and delivery traveling salesman problem with first-in-first-out loading. *Computers & Operations Research* 36(6):1800–1808.
- Falcon R, Li X, Nayak A, Stojmenovic I (2010) The one-commodity traveling salesman problem with selective pickup and delivery: An ant colony approach. *IEEE Congress on Evolutionary Computation*, 1–8 (IEEE).
- Fazi S, Fransoo JC (2025) Freight mobility as a service: Open platforms for synchro-modal transport. *Transportation Research Part E: Logistics and Transportation Review* 204:104368.
- Feillet D, Dejax P, Gendreau M (2005) Traveling salesman problems with profits. *Transportation science* 39(2):188–205.
- Gao C, Wei N, Walteros JL (2023) An exact approach for solving pickup-and-delivery traveling salesman problems with neighborhoods. *Transportation Science* 57(6):1560–1580.
- Ghilas V, Demir E, Van Woensel T (2016) An adaptive large neighborhood search heuristic for the pickup and delivery problem with time windows and scheduled lines. *Computers & Operations Research* 72:12–30.
- Gribkovskaia I, Halskau sr Ø, Laporte G, Vlček M (2007) General solutions to the single vehicle routing problem with pickups and deliveries. *European Journal of Operational Research* 180(2):568–584.
- Gribkovskaia I, Laporte G, Shyshou A (2008) The single vehicle routing problem with deliveries and selective pickups. *Computers & Operations Research* 35(9):2908–2924.
- Hernández-Pérez H, Salazar-González JJ (2003) The one-commodity pickup-and-delivery travelling salesman problem. *Combinatorial Optimization—Eureka, You Shrink! Papers Dedicated to Jack Edmonds 5th International Workshop Aussois, France, March 5–9, 2001 Revised Papers*, 89–104 (Springer).
- Hernández-Pérez H, Salazar-González JJ (2009) The multi-commodity one-to-one pickup-and-delivery traveling salesman problem. *European Journal of Operational Research* 196(3):987–995.
- Hernández-Pérez H, Salazar-González JJ (2014) The multi-commodity pickup-and-delivery traveling salesman problem. *Networks* 63(1):46–59.
- Jerebic J, Mernik M, Liu SH, Ravber M, Baketarić M, Mernik L, Črepinšek M (2021) A novel direct measure of exploration and exploitation based on attraction basins. *Expert Systems with Applications* 167:114353.
- Kalantari B, Hill AV, Arora SR (1985) An algorithm for the traveling salesman problem with pickup and delivery customers. *European Journal of Operational Research* 22(3):377–386.
- Kassoumeh AK, Kartal Z, Arslan A (2025) The effect of different initial solutions on the metaheuristic algorithms for the single allocation p-hub center and routing problem. *PeerJ Computer Science* 11:e2840.
- Kong D, Ma Y, Cao Z, Yu T, Xiao J (2024) Efficient neural collaborative search for pickup and delivery problems. *IEEE Transactions on Pattern Analysis and Machine Intelligence* .
- Kool W, Van Hoof H, Welling M (2018) Attention, learn to solve routing problems! *arXiv preprint arXiv:1803.08475* .

- Kwon YD, Choo J, Kim B, Yoon I, Gwon Y, Min S (2020) Pomo: Policy optimization with multiple optima for reinforcement learning. *Advances in Neural Information Processing Systems* 33:21188–21198.
- Laporte G, Martello S (1990) The selective travelling salesman problem. *Discrete applied mathematics* 26(2-3):193–207.
- Li J, Xin L, Cao Z, Lim A, Song W, Zhang J (2021) Heterogeneous attentions for solving pickup and delivery problem via deep reinforcement learning. *IEEE Transactions on Intelligent Transportation Systems* 23(3):2306–2315.
- Liu S, Sun J, Duan X, Liu G (2024) Parallel adaptive large neighborhood search based on spark to solve vrptw. *Scientific Reports* 14(1):23809.
- Ma Y, Li J, Cao Z, Song W, Guo H, Gong Y, Chee YM (2022) Efficient neural neighborhood search for pickup and delivery problems. *arXiv preprint arXiv:2204.11399*.
- Ma Y, Li J, Cao Z, Song W, Zhang L, Chen Z, Tang J (2021) Learning to iteratively solve routing problems with dual-aspect collaborative transformer. *Advances in Neural Information Processing Systems* 34:11096–11107.
- Masson R, Lehuédé F, Péton O (2013) An adaptive large neighborhood search for the pickup and delivery problem with transfers. *Transportation Science* 47(3):344–355.
- Mosheiov G (1994) The travelling salesman problem with pick-up and delivery. *European Journal of Operational Research* 79(2):299–310.
- Pisinger D, Ropke S (2018) Large neighborhood search. *Handbook of metaheuristics*, 99–127 (Springer).
- Psaraftis HN (1980) A dynamic programming solution to the single vehicle many-to-many immediate request dial-a-ride problem. *Transportation Science* 14(2):130–154.
- Ropke S, Pisinger D (2006) An adaptive large neighborhood search heuristic for the pickup and delivery problem with time windows. *Transportation science* 40(4):455–472.
- Salazar-González JJ, Santos-Hernández B (2015) The split-demand one-commodity pickup-and-delivery travelling salesman problem. *Transportation Research Part B: Methodological* 75:58–73.
- Shaw P (1998) Using constraint programming and local search methods to solve vehicle routing problems. *International conference on principles and practice of constraint programming*, 417–431 (Springer).
- Sun Z, Yang Y (2023) Difusco: Graph-based diffusion solvers for combinatorial optimization. *Advances in neural information processing systems* 36:3706–3731.
- Ting CK, Liao XL (2013) The selective pickup and delivery problem: Formulation and a memetic algorithm. *International Journal of Production Economics* 141(1):199–211.
- Van der Bruggen L, Lenstra JK, Schuur P (1993) Variable-depth search for the single-vehicle pickup and delivery problem with time windows. *Transportation Science* 27(3):298–311.
- Vaswani A, Shazeer N, Parmar N, Uszkoreit J, Jones L, Gomez AN, Kaiser L, Polosukhin I (2017) Attention is all you need. *Advances in neural information processing systems* 30.

- Veenstra M, Roodbergen KJ, Vis IF, Coelho LC (2017) The pickup and delivery traveling salesman problem with handling costs. *European Journal of Operational Research* 257(1):118–132.
- Vinyals O, Fortunato M, Jaitly N (2015) Pointer networks. *Advances in neural information processing systems* 28.
- Wu X, Wang D, Wen L, Xiao Y, Wu C, Wu Y, Yu C, Maskell DL, Zhou Y (2024) Neural combinatorial optimization algorithms for solving vehicle routing problems: A comprehensive survey with perspectives. *arXiv preprint arXiv:2406.00415* .
- Xin L, Song W, Cao Z, Zhang J (2021) Neurokh: Combining deep learning model with lin-kernighan-helsgaun heuristic for solving the traveling salesman problem. *Advances in Neural Information Processing Systems* 34:7472–7483.

This publication is part of the project FMaaS - it's a cargo match (with project number NWA.1518.22.023) of the research programme Dutch Research Agenda - research along NWA routes by consortia which is (partly) financed by the Dutch Research Council (NWO).

Appendices

7 Additional Methodology Details

7.1 Mixed Integer Linear Programming

We formulate a MILP that maximizes total collected revenue. The model explicitly encodes precedence, capacity, and route-length constraints and supports exact solution and bounding methods. Solving the MILP provides a ground-truth reference for evaluating heuristics on small instances.

Decision variables: For every two distinct vertices $i, j \in \mathcal{V}$, let $X_{ij} \in \{0, 1\}$ indicate whether edge (i, j) is visited, let i_h denote the pickup vertex of request $h \in \mathcal{H}$, let $T_i \geq 0$ denote the cumulative length from vehicle's start vertex 0 to vertex i along the selected route, and $L_i \geq 0$ the load on departure from vertex i .

$$\min \quad - \sum_{h \in \mathcal{H}} r_h \left(\sum_{j \in \mathcal{V}} X_{i_h j} \right) \quad (11)$$

$$\text{s.t.} \quad X_{ii} = 0, \quad \forall i \in V, \quad (12)$$

$$\sum_{j \in \mathcal{P}} X_{0j} = 1, \quad \sum_{i \in \mathcal{D}} X_{i, 2n+1} = 1, \quad (13)$$

$$\sum_{i \in V} X_{i0} = 0, \quad \sum_{j \in V} X_{2n+1, j} = 0, \quad (14)$$

$$\sum_{j \in V} X_{ij} = \sum_{j \in V} X_{ji}, \quad \forall i \in \mathcal{P} \cup \mathcal{D}, \quad (15)$$

$$\sum_{j \in V} X_{ij} \leq 1, \quad \forall i \in V \setminus \{2n+1\}, \quad (16)$$

$$\sum_{i \in V} X_{ij} \leq 1, \quad \forall j \in V \setminus \{0\}, \quad (17)$$

$$\sum_{j \in V} X_{ij} = \sum_{j \in V} X_{j, i+n}, \quad \forall i \in \mathcal{P}, \quad (18)$$

$$T_0 = 0, \quad T_{2n+1} \leq T, \quad (19)$$

$$X_{ij} = 1 \Rightarrow T_j \geq T_i + c_{ij}, \quad \forall i, j \in V, i \neq j, \quad (20)$$

$$\sum_{j \in V} X_{ij} = 1 \Rightarrow T_{i+n} \geq T_i, \quad \forall i \in \mathcal{P}, \quad (21)$$

$$L_0 = 0, \quad 0 \leq L_i \leq Q, \quad \forall i \in V, \quad (22)$$

$$X_{ij} = 1 \Rightarrow L_j = L_i + q_j, \quad \forall i \in V, j \in \mathcal{P}, \quad (23)$$

$$X_{ij} = 1 \Rightarrow L_j = L_i - q_{j-n}, \quad \forall i \in V, j \in \mathcal{D}, \quad (24)$$

$$L_{2n+1} = 0, \quad (25)$$

$$X_{ij} \in \{0, 1\}, \quad \forall i, j \in V, i \neq j, \quad (26)$$

$$T_i \geq 0, L_i \geq 0, \quad \forall i \in V. \quad (27)$$

Constraint explanations: Objective (11) minimizes the negative collected revenue. Start/end anchoring (13)–(14) and flow/selectivity (15)–(17) enforce a single path that visits each vertex at most once. Pairing (18) and precedence (21) ensure a request is served if and only if both pickup and delivery are included and the pickup precedes the delivery (in cumulative-length order). Length-compatibility (20) ties visited arcs to cumulative length and, with positive arc lengths, eliminates subtours; (19) caps total route length. Capacity bounds (22) with load propagation (23)–(24) maintain feasible loads; (25)–(27) set terminal load and variable domains.

7.2 Attention Mechanism

In the encoder, each node’s hidden state \mathbf{h}_i is first projected into three distinct representations: queries \mathbf{q}_i , keys \mathbf{k}_i and values \mathbf{v}_i by multiplying with learnable weight matrices W^Q , W^K and W^V . The query and key projections both map the original embedding (dimension $d_{\mathbf{h}}$) into a d_k -dimensional space, while the value projection maps into a d_v -dimensional space. Intuitively, \mathbf{q}_i represents what node i “asks” of its neighbors, \mathbf{k}_j represents how node j “presents” itself to be attended, and \mathbf{v}_j is the actual information node j contributes once its key matches a query. We define dimensions d_k and d_v and compute the query $\mathbf{q}_i \in \mathbb{R}^{d_k}$, key $\mathbf{k}_i \in \mathbb{R}^{d_k}$, value $\mathbf{v}_i \in \mathbb{R}^{d_v}$ for each node by projecting the embedding $\mathbf{h}_i^{(\ell)}$ for all $\ell \in \{1, \dots, L\}$ as $\mathbf{q}_i^{(\ell)} = W^Q \mathbf{h}_i^{(\ell)}$, $\mathbf{k}_i^{(\ell)} = W^K \mathbf{h}_i^{(\ell)}$, $\mathbf{v}_i^{(\ell)} = W^V \mathbf{h}_i^{(\ell)}$. Here parameters W^Q and W^K are $d_k \times d_{\mathbf{h}}$ matrices and W^V is a $d_v \times d_{\mathbf{h}}$ matrix.

When computing the updated representation for node i , we form the compatibility between \mathbf{q}_i and each neighbor’s key \mathbf{k}_j via their dot product, scaled by $1/\sqrt{d_k}$ to prevent the magnitudes from growing too large as dimensionality increases. These scores are optionally masked and then passed through a softmax function across all nodes $j \in V$, yielding a distribution of attention weights.

$$\mathbf{h}'_i = \sum_j \text{softmax} \left(\frac{\mathbf{q}_i^{(\ell)\top} \mathbf{k}_j^{(\ell)}}{\sqrt{d_k}} \odot \mathcal{M}_t \right) \mathbf{v}_j^{(\ell)}, \quad (28)$$

where $d_k = \frac{d_{\mathbf{h}}}{M}$ is the query and key dimensionality, \odot denotes the Hadamard (element-wise) product and \mathcal{M}_t is the mask matrix. The new vector \mathbf{h}'_i is simply the weighted sum of the neighbors’ value vectors, so that nodes with keys most aligned to the query of node i contribute more heavily to its updated embedding.

Multi-Head Attention: To capture multiple types of interactions simultaneously, the model splits the projections into M separate heads. In each head m , its own triplet of weight matrices W_m^Q , W_m^K and W_m^V computes a head-specific output \mathbf{h}'_{im} with $d_k = d_v = \frac{d_{\mathbf{h}}}{M} = 16$. These $M = 8$ head outputs are then linearly projected back to the original hidden size $d_{\mathbf{h}}$ via head-specific matrices W_m^O , and summed. This multi-head architecture allows different subspaces to specialize, for instance one head focusing on content information while another

captures positional relationships.

$$\mathbf{MHA}_i(\mathbf{h}_1, \dots, \mathbf{h}_n) = \sum_{m=1}^M W_m^O \mathbf{h}'_{im}. \quad (29)$$

Feed-Forward Sublayer: Following the attention mechanism, each node’s representation passes through a two-layer feed-forward network applied independently to each position. The first linear layer expands the dimension from $d_{\mathbf{h}}$ up to a larger hidden size $d_{\text{ff}} = 512$, applies a ReLU activation function, and consequently projects back down to $d_{\mathbf{h}}$. This position-wise MLP enriches each node’s features with non-linear combinations of the attention output, enabling the network to model complex interactions that attention alone cannot capture.

$$\mathbf{FF}(\hat{\mathbf{h}}_i) = W^{\text{ff},1} \cdot \text{ReLU}(W^{\text{ff},0} \hat{\mathbf{h}}_i + \mathbf{b}^{\text{ff},0}) = \mathbf{b}^{\text{ff},1}. \quad (30)$$

Batch Normalization Batch normalization is applied to stabilize training. For each feature dimension, the activations across the batch are normalized to zero mean and unit variance, then rescaled and shifted by learned parameters w^{bn} and b^{bn} . This normalization occurs after the feed-forward sublayer, smoothing out differences in scale across training examples and allowing for higher learning rates.

$$\mathbf{BN}(\mathbf{h}_i) = w^{\text{bn}} \odot \overline{\mathbf{BN}}(\mathbf{h}_i) + \mathbf{b}^{\text{bn}}, \quad (31)$$

where $\overline{\mathbf{BN}}$ refers to batch normalization without affine transformation.

7.3 Traing Algorithm

Given an instance $s = (f, \mathcal{F}) \in \mathcal{S}_{\mathcal{X}}$, the objective is to find the optimal solution for $\pi^* = \arg \min_{\pi \in \mathcal{F}} f(x)$. Probabilistic COP solvers tackle instance problems by parameterizing the solution space with a continuous and differentiable vector $\boldsymbol{\theta}$ and defining $p_{\boldsymbol{\theta}}(\pi|s)$ a parameterized conditional distribution over discrete feasible complete solutions $\pi \in \mathcal{F}$. The goal is to minimize the expected negative collected revenues under $p_{\boldsymbol{\theta}}$ given by

$$\mathcal{L}(\boldsymbol{\theta}|s) = \mathbb{E}_{\pi \sim p_{\boldsymbol{\theta}}(\cdot|s)}[f(\pi)] = \sum_{\pi \in \mathcal{F}} p_{\boldsymbol{\theta}}(\pi|s) f(\pi). \quad (32)$$

Reinforcement learning (RL) algorithms can be applied as a gradient estimator to optimize such probabilistic generative models. The gradient of (32) can be formulated using the well-known REINFORCE algorithm:

$$\nabla_{\boldsymbol{\theta}} \mathcal{L}(\boldsymbol{\theta}|s) = \mathbb{E}_{\pi \sim p_{\boldsymbol{\theta}}(\cdot|s)}[(f(\pi) - b(s)) \nabla_{\boldsymbol{\theta}} \log p_{\boldsymbol{\theta}}(\pi|s)], \quad (33)$$

where $b(s)$ denotes a baseline function that does not depend on π and estimates the expected negative collected revenues to reduce the variance of the gradients. This estimator is unbiased and does not require differentiable dynamics

or rewards, making it suitable for discrete, non-differentiable combinatorial decisions.

During training, the problem instances are independently and identically distributed (i.i.d.) drawn from a distribution \mathbb{S} , so that the total training objectives involves sampling from the distribution of instances, i.e., $\mathcal{L}(\boldsymbol{\theta}) = \mathbb{E}_{s \in \mathbb{S}} \mathcal{L}(\boldsymbol{\theta}|s)$. By drawing B i.i.d. sample instances $s_1, s_2, \dots, s_B \sim \mathbb{S}$ and sampling a single feasible complete solution per instance, i.e., $\pi_i \sim p_{\boldsymbol{\theta}}(\cdot|s_i)$, the gradient in (33) can be approximated via Monte Carlo sampling (average the score-function terms):

$$\nabla_{\boldsymbol{\theta}} \mathcal{L}(\boldsymbol{\theta}|s) \approx \frac{1}{B} \sum_{i=1}^B \left(f(\pi_i) - b(s_i) \right) \nabla_{\boldsymbol{\theta}} \log p_{\boldsymbol{\theta}}(\pi_i|s_i), \quad (34)$$

The whole training procedure of AM (Kool et al. 2018) is summarized in Alg. 3.

Algorithm 3 REINFORCE with Rollout Baseline

```

1: Input: number of epochs  $E$ , steps per epoch  $T$ , batch size  $B$ , significance  $\alpha$ 
2: Initialize  $\boldsymbol{\theta}, \boldsymbol{\theta}^{\text{BL}} \leftarrow \boldsymbol{\theta}$ 
3: for epoch = 1, ...,  $E$  do
4:   for step = 1, ...,  $T$  do
5:      $s_i \leftarrow \text{RANDOMINSTANCE}() \quad \forall i \in \{1, \dots, B\}$ 
6:      $\pi_i \leftarrow \text{SAMPLEROLLOUT}(s_i, p_{\boldsymbol{\theta}}) \quad \forall i \in \{1, \dots, B\}$ 
7:      $\pi_i^{\text{BL}} \leftarrow \text{GREEDYROLLOUT}(s_i, p_{\boldsymbol{\theta}^{\text{BL}}}) \quad \forall i \in \{1, \dots, B\}$ 
8:      $\nabla \mathcal{L} \leftarrow \frac{1}{B} \sum_{i=1}^B \left( f(\pi_i) - f(\pi_i^{\text{BL}}) \right) \nabla_{\boldsymbol{\theta}} \log p_{\boldsymbol{\theta}}(\pi_i)$ 
9:      $\boldsymbol{\theta} \leftarrow \text{ADAM}(\boldsymbol{\theta}, \nabla \mathcal{L})$ 
10:   if  $\text{ONESIDEDPAIREDTTTEST}(p_{\boldsymbol{\theta}}, p_{\boldsymbol{\theta}^{\text{BL}}}) < \alpha$  then  $\boldsymbol{\theta}^{\text{BL}} \leftarrow \boldsymbol{\theta}$ 

```

7.4 Definition of Solution Space

Let \mathcal{X} denote the set of all possible and feasible *partial solutions* for a given COP, $\mathcal{F} \in \mathcal{X}$. Let \mathcal{Z} be the set of *elementary construction steps* (adding one pickup vertex, one delivery vertex or the end vertex z^e). A solution is a finite sequence of steps. We assume that \mathcal{X} is equipped with a concatenation operator \circ (for a sequence $x = z_1 \circ \dots \circ z_k$ and a step $z \in \mathcal{Z}$, $x \circ z := z_1 \circ \dots \circ z_k \circ z$) having a neutral element ϵ (empty sequence) such that $\epsilon \circ x = x$. For a sequence $\mathbf{z}_{1:k} = z_1 \circ \dots \circ z_k$ with $k \geq 1$ and $\mathbf{z}_{1:k} \in \mathcal{Z}^k$, the set of partial solutions is $\mathcal{X} = \{\mathbf{z}_{1:k} : C(\mathbf{z}_{1:\ell}) = \text{T} \quad \forall \ell \leq k\}$. For any $x \in \mathcal{X}$, we define its *admissible step set* as

$$A(x) := \{z \in \mathcal{Z} : C(x \circ z) = \text{T}\}.$$

A partial solution $x \in \mathcal{X}$ is *complete* if and only if no admissible step remains,

$$x \text{ is complete} \iff A(x) = \emptyset.$$

We define $(\mathcal{X}, \circ, \epsilon, \mathcal{Z})$ as the solution space.

For the *mI-PDSTSP*, operator \circ is the sequence concatenation, ϵ is the empty sequence including trivial route at the vehicle's start vertex 0, and the step is a sequence of length 1. The predicate $C(\mathbf{z}_{1:\ell}) = \text{T}$, where $\mathbf{z}_{1:\ell} \in \mathcal{Z}^{\ell}$,

is interpreted as a *closure guarantee*: there exists at least one finite extension that serves all pending deliveries and terminates at the end vertex $z^e = 2n+1$. Formally,

$$C(\mathbf{z}_{1:\ell}) = \text{T} \implies \exists y \in \mathcal{Z}^* \text{ s. t. } \mathbf{z}_{1:\ell} \circ y \circ z^e \in \mathcal{F},$$

where y is a concatenation of the outstanding delivery steps (in some order) and \mathcal{Z}^* denotes the set of all finite sequences of all outstanding delivery steps. A partial solution x is feasible and complete if and only if it reaches vertex $2n+1$ while satisfying all operational constraints (capacity, route-length, and pickup-delivery precedence) at every prefix. Consequently, any feasible, complete solution is a composition of admissible steps starting from ϵ (vertex 0) and ending at vertex $2n+1$. The problem thus reduces to selecting a sequence $(z_1, \dots, z_\tau = z^e)$ with $z_\ell \in A(\mathbf{z}_{1:\ell-1})$ for all $\ell \leq \tau$, such that $\mathbf{z}_{1:\tau} \in \arg \min_{x \in \mathcal{F}} f(x)$, a task which can naturally be modeled as an Markov decision process (MDP).

7.5 Markov Decision Process for Improvers

The MDP for improvers has the same solution space \mathcal{F} but different state space $\bar{\mathcal{X}} := x \in \mathcal{F}$, action space $\mathcal{A} := \{a \in A(x)\} \cup \{\epsilon\}$, where $A(x)$ is the set of admissible step such that $x \xrightarrow{z} x'$ for all $z \in A(x)$ where $x' \in \mathcal{F}$ and $|x| < |x'|$. The labelled transition system is $x \xrightarrow[z]{f(x)-f(x')} x'$ and the reward function is $r(x, z) = f(x) - f(x')$.

8 Details of Baselines

We compare our MSLNS algorithm with several baselines. Tab. 4 introduces the baseline decoders first, describing their main strategies and hyperparameters, and lists the combinatorial optimization (CO) post-improvement operators that can be applied on top of a decoder, together with their configurations. We also provide the computational complexity of all baselines and improvement operators in Tab. 4.

Since the effectiveness of different decoders (e.g., BS, MS, sampling) is largely determined by the number of candidate trajectories explored, we equalize their hyperparameters (e.g., setting $\beta = M = n/2$) to align computational budgets and prevent artificial advantages. Similarly, when comparing improvers (BI-LNS, LNS, MSLNS, SA), which may not converge within a fixed time budget, we equalize their time budgets (e.g., $t_{\max} = 1\text{s}$) to ensure a fair comparison.

Simulation-guided Beam Search (SGBS) is a beam search-based constructing algorithm proposed by Choo et al. (2022) that examines candidate solutions within a fixed-width tree search that both a DNN-learned policy and a simulation (rollout) identify as promising. Given that SGBS is designed for unselective routing problems, we customize it for the *m1-PDSTSP*. Similar to MSLNS, after each step, before selecting the top β candidate routes, we remove

Table 4: Baselines descriptions

Algorithm	Description	Hyperparameters	Complexity
Baselines			
AM	Greedy decoding strategy of the AM	-	$\mathcal{O}(n^2L)$
AM-sample	Sampling decoding strategy of the AM	$\eta \in \{n/2, 100\}$ samples	$\mathcal{O}(\eta n^2L)$
AM-BS	Beam Search decoding strategy of the AM	beam width $\beta \in \{n/2, 100\}$	$\mathcal{O}(\beta n^2L)$
AM-MS	Multi-Start greedy trajectories of the AM	$M = n/2$	$\mathcal{O}(M n^2L)$
POMO-single	Single greedy trajectory of POMO	-	$\mathcal{O}(n^2L)$
POMO	Multi greedy trajectories of POMO	$M = n/2$	$\mathcal{O}(M n^2L)$
POMO-SGBS	SGBS (Choo et al. 2022) combined with POMO	$\beta = \gamma = 5$	$\mathcal{O}(\beta \gamma n^2L)$
Gurobi	Gurobi solver v12.0.3	-	-
GS	Greedy Search heuristic	-	$\mathcal{O}(n)$
MSG	Multi-Start Greedy Search heuristic	$M = n/2$	$\mathcal{O}(M n)$
LNS	Large Neighborhood Search with random destroy	time out $t_{max} \in \{1s, 4s, 10s\}$ or iteration I	$\mathcal{O}(I n^3)$
SA	Simulated Annealing	time out $t_{max} \in \{1s, 4s, 10s\}$	-
Post-improvement CO operators			
2-Opt	Local 2-Opt refinement operator	until no gain	$\mathcal{O}(n^2)$
HC	Hill Climbing on neighborhood	until no gain	$\mathcal{O}(n^3)$
1-LNS	1-destroy Best-improvement LNS	time out $t_{max} \in \{1s, 4s, 10s\}$	$\mathcal{O}(n^4)$
MSLNS	Multi-Start Large Neighborhood Search	$M \in [5, 10], \beta \in [3, 5], t_{max} \in \{1s, 4s, 10s\}$	$\mathcal{O}(n/k_{max}) M n^3$

L is the layer size of Transformer decoder. For baselines, we do not include masking costs in the complexity analysis.

the duplicated routes (routes with same selected requests set) to ensure diversity. During the beam search, the rollout simulation is performed using the greedy decoding strategy of the POMO model as in Alg. 4.

Algorithm 4 Policy Optimization with Multiple Optima Inference

- 1: **Input:** instance s , policy p_θ , number of start pickup nodes per sample M
 - 2: $\{\pi_1^1, \pi_1^2, \dots, \pi_1^M\} \leftarrow \text{SelectStartPickupNodes}(s)$
 - 3: $\pi^j \leftarrow \text{GreedyRollout}(\pi_1^j, s, p_\theta) \quad \forall j \in \{1, \dots, M\}$
 - 4: $j_{min} \leftarrow \arg \min_{j \in \{1, \dots, M\}} f(\pi^j)$
 - 5: **return** $\pi^{j_{min}}$
-

Greedy Search is a constructor that iteratively selects the option that offers the most immediate benefit at each step, without regard for future consequences. We design the GS algorithm based on the problem structure. Each new node is chosen based on fitness, which is defined as follow:

$$\text{fitness}_j = r_j - c_{i,j}, \quad \forall j \in \mathcal{V}. \quad (35)$$

Multi-Start Greedy Search is an extension of GS that generates multiple initial solutions by varying the M starting pickup nodes based on (35), and selects the best among them.

Large Neighborhood Search is an improver that iteratively destroys a portion of the current solution and repairs it to explore a larger solution neighborhood. To implement LNS for $m1$ -PDSTSP, we employ the random destroy ($k \sim \text{Unif}\{1, \dots, k_{max}\}$ requests drawn uniformly at random) and greedy insertion repair strategies (Alg. 5). The complexity of REPAIR is $\mathcal{O}(n^3)$. Through our experiments, we find that $k_{max} = 3$ generates the best performance.

Algorithm 5 REPAIR/Greedy Insertion

Require: route π^* , instance size n , load list q , capacity limit Q , maximum length limit T , reward function f

- 1: **while** $\pi^* = \pi$ **do**
- 2: $\pi \leftarrow \pi^*$
- 3: Compute remaining capacity cap_left along route π
- 4: Initialize $ValidRoutes \leftarrow \{\pi\}$, $Scores \leftarrow \{R(\pi)\}$
- 5: **for** request $r = 0$ to $n - 1$ where $r \notin \pi$ **do**
- 6: $Intervals \leftarrow \text{FINDCAPACITYGAP}(Q - cap_left - q[r])$
- 7: **for** each interval $[s, e] \in Intervals$ **do**
- 8: $candidates \leftarrow \text{INSERT}([s, e], r, r + n)$ \triangleright There can be multiple candidates
- 9: **for** each $cand \in candidates$ **do**
- 10: **if** Route length $c(cand) \leq T$ **then**
- 11: Append $cand$ to $ValidRoutes$ and $R(cand)$ to $Scores$
- 12: $\pi^* \leftarrow ValidRoutes[\arg \max Scores]$
- 13: **return** π^*

Simulated Annealing is an improver that occasionally accepts worse moves with probability $e^{-\Delta/\text{temperature}}$ under a cooling schedule to escape local optima. To implement SA for the *m1-PDSTSP*, traditional operators like INVERSE, SWAP, and INSERT_SUBTOUR cannot be directly applied due to stringent constraints. Particularly, INSERT_SUBTOUR almost always violates nearly all constraints when a subsequence is randomly repositioned. Because the route visits only a subset of nodes, we treat INSERT as adding a new request (pickup-delivery pair) rather than deleting and reinserting existing nodes. As for the INVERSE operator, its application is generally restricted to changing the order among groups of consecutive pickup or delivery nodes. Effectively, this becomes a SWAP operation when only two consecutive nodes are reordered. SWAP also allows for the repositioning of a pickup node from one request with a delivery node from another. Therefore, we can only keep the SWAP operator and abandon the INVERSE.

In addition to adapting the INSERT and SWAP operators, a new operator called REPLACE can be introduced. This operator allows for the replacement of the pickup-delivery pair nodes of a selected request with those of an unselected request in the same positions in the route. Furthermore, we can introduce a DESTROY operator, which randomly removes a selected request from the route. We set the hyperparameters as follows: initial temperature is 10, cooling rate is 0.95, stopping temperature is 0.01 and the number of iterations for each temperature is 20.

8.1 Details of Improvers

2-Opt is an improver that repeatedly selects two edges in a tour, reverses the intervening segment (swapping the edges), and keeps the change if the new route is feasible and shortens the route, until no further improvement is possible.

Hill Climbing is an improver that starts with an initial solution and iteratively makes small changes to improve it. The algorithm examines neighboring solutions and moves to a neighbor that offers an improvement (i.e., Alg. 5) over the current one. This process repeats until no further improvements can be found.

Best-improvement Large Neighborhood Search is an improver that starts from an initial solution, iteratively enumerates all neighbors and picks the best, repeatedly moving to an improving neighbor. The process continues until no improving move is found or a predefined stopping criterion is met. In this paper, we implement a 1-destroy BI-LNS that selects only one requests in the current solution to destroy and reinsert the destroyed solution greedily (Alg. 5). This reinsertion process repeats until no single-request reinsertion yields improvement.

9 Additional Revenue Settings

9.1 Revenue Settings

We have experimented with four different revenue settings to evaluate the robustness of our method. The details of the *Ton-Distance*, *Constant* and *Uniform* settings are described below.

1. **Ton-Distance:** This setting rewards requests in proportion to the product of demand and pickup-delivery separation. $r_h = q_h \cdot c_{h,h+n} * \mu$, where $\mu \sim \text{Unif}(0.5, 1.5)$ is the discount to add randomness, $\hat{r}_h = \frac{r_h}{\max\{r_h\}}$. Ton-Distance is a standard industry metric that reflects both the weight and distance of freight, aligning with how carriers are often paid and how costs are incurred.
2. **Constant:** Every node has the same revenue, therefore, the goal becomes to maximize the number of served customers within the maximum length constraint. $r_h = \hat{r}_h = 1$.
3. **Uniform:** The revenue of each request is uniformly sampled from the set $\{1, 2, \dots, 100\}$. $r_h \sim \text{Uniform}(1, 100)$, $\hat{r}_h = \frac{r_h}{100}$. This setting introduces variability in revenues, reflecting scenarios where different requests have different levels of importance or urgency.

10 Additional Experimental Results

10.0.1 More details on Distance m1-PDSTSP

Given AM, POMO and multiple baselines with numerous hyperparameters, we first tune all methods on PDSTSP42 under the *Distance* setting. Hyperparameters are selected using a validation split, and the best methods choice is made

on the Pareto frontier of revenue (higher is better) versus computational cost (lower is better) in Fig. 6.

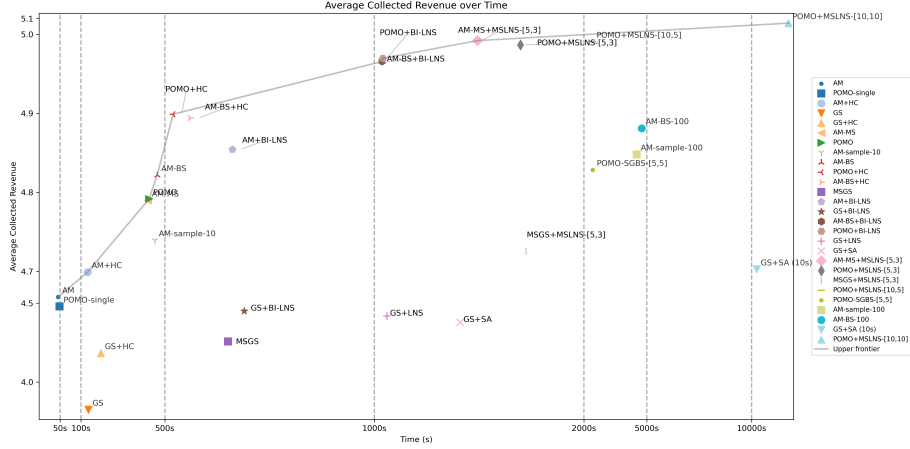


Figure 6: Average collected revenue vs. wall-clock time for all contenders on PDSTSP42. Each marker denotes a method; x-axis is runtime (vertical dashed lines indicate time budgets) and y-axis is mean revenue. The Pareto front is traced by AM/AM+HC (low), POMO+HC (middle), POMO/AM+MSLNS $_{10,5}^{t_{max}}$ and POMO/AM-BS+BI-LNS $^{t_{max}}$ (high), and POMO+MSLNS $_{10,10}$ (higher).

From Fig. 6, a clear Pareto front emerges. For small budgets ($\leq 100s$), AM+HC dominates the quick region (≈ 4.7 avg revenue), outperforming GS, HC, AM, and POMO-single. In the mid-budget range $500 - 1000s$, AM-BS improves a bit (≈ 4.8) but is soon dominated by POMO+HC and AM-BS+HC. In the high-budget range ($200s - 5000s$), time-limited LNS-based and MSLNS-based hybrids give a significant jump (≈ 5.0), beating LNS/SA and heavy sampling/beam-search/SGBS variants. For higher budgets ($\geq 3000s$), POMO+MSLNS $_{10,10}$ is at the top (≈ 5.1). Fig. 7 shows routes generated by POMO, POMO+BI-LNS $^{t_{max}}$, MSLNS $_{10,5}^{t_{max}}$ and POMO+MSLNS $_{10,10}$ for 9 random instances.

10.0.2 Different maximum route-lengths

We evaluate the performance of different methods under various maximum length sizes T for the *Distance* setting to understand how route-length constraints impact solution quality. We consider three sizes: tight ($T = 2$), medium ($T = 4$), and large ($T = 8$) with fixed capacity ($Q = 10$), which correspond to different levels of route-length tightness. For each size, we report the average revenue achieved by each method on the test set of 1,000 instances.

Across both sizes (PDSTSP42 and PDSTSP82 in Tab. 5) and all gap classes (Tight/Middle/Wide), hybrid methods that start from NCO solutions and apply search consistently dominate pure baselines. Single-shot baselines (AM, POMO,

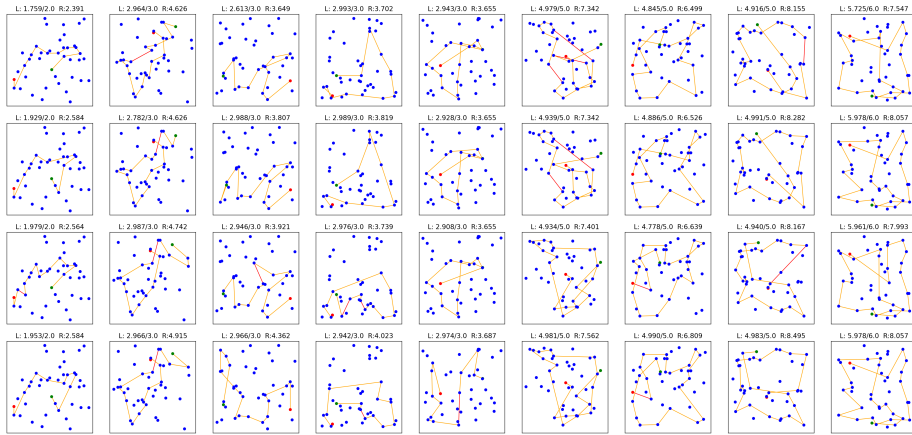


Figure 7: Example routes on *Distance* PDSTSP42 with Q and T randomly generated. Top to bottom: POMO, POMO+BI-LNS $^{t_{max}}$, POMO+MSLNS $^{t_{max}}_{[10,5]}$, and POMO+MSLNS $_{[10,10]}$.

and POMO-single) are clearly behind. Adding search to AM/POMO helps a lot: AM-BS, AM-MS, and POMO close much of the gap, and adding improver give another solid boost. Except for the unlimited POMO+MSLNS $_{[10,10]}$, its time-budgeted sibling POMO+MSLNS $^{t_{max}}_{[10,5]}$ is a practical substitute, reaching within $\approx 0.5 - 1.5\%$ of the best with far less time. We see POMO+MSLNS $^{t_{max}}_{[10,5]}$ is only surpassed by POMO+BI-LNS $^{t_{max}}$ on wide PDSTSP82 as wide gaps on larger instances demand more destroy-repair time, and the multi-start variant can hit the budget before fully exploring. Finally, the WR columns on PDSTSP82 suggest AM-BS families often win on Middle/Wide, indicating AM-BS and POMO explore complementary regions of the solution space.

10.0.3 Generalization experiments

We assess out-of-distribution (OOD) generalization by training (and tuning hyperparameters) on a *source* distribution and evaluating *without further training* on a *target* distribution that differs in problem factors. Concretely, we vary instance scale n , models trained at PDSTSP42 are evaluated at PDSTSP82 and PDSTSP122, and models trained at PDSTSP82 are evaluated at PDSTSP122. We report zero-shot performance, which demonstrates how well our model performs on a new task or distribution without any additional training on that target. This protocol quantifies robustness to scale/distribution shift, helps detect overfitting, and guides design choices. In practice, problem scale and mix evolve over time (new regions, more customers, seasonal peaks), and retraining for every shift is rarely feasible; zero-shot evaluation thus indicates how reliable and robust a method is.

Based on the results in Tab. 6 and Tab. 3, we observe that all methods expe-

Table 5: Performance matrix: PDSTSP42 vs. PDSTSP82 across gap classes (Tight/Middle/Wide) on the *Distance* setting with $Q = 10$.

		PDSTSP42					PDSTSP82				
Algorithm		Time	Revenue	Length	Gap	WR	Time	Revenue	Length	Gap	WR
Tight ($T = 2$)	GS+BNS ^{t_{max}}	2m	1.686	1.933	12.51%	32.1%	4m	2.031	1.952	15.69%	18.4%
	POMO-single	9s	1.581	1.876	18.09%	14.2%	21s	1.936	1.903	19.63%	5.5%
	AM	8s	1.668	1.877	13.45%	21.5%	27s	2.039	1.902	15.36%	10.2%
	AM-MS	1m	1.815	1.911	5.80%	39.7%	5m	2.265	1.932	5.98%	22.9%
	POMO	1m	1.820	1.896	5.49%	40.8%	5m	2.263	1.935	6.06%	26.1%
	AM-BS	1m	1.847	1.917	4.03%	53.2%	6m	2.315	1.942	3.90%	40.5%
	POMO+BNS ^{t_{max}}	3m	1.874	1.938	2.74%	63.4%	10m	2.335	1.944	3.07%	49.4%
	AM-BS+BNS ^{t_{max}}	3m	1.886	1.929	2.12%	70.3%	11m	2.356	1.948	2.20%	56.8%
	POMO+MNS ^{t_{max}} _[10,5]	15m	1.915	1.931	0.64%	87.3%	42m	2.396	1.948	0.53%	77.8%
	POMO+MNS _[10,10]	30m	1.919	1.933	0.41%	91.8%	1.4h	2.409	1.951	0.00%	89.6%
Gurobi	20.0h	1.927	1.956	0.00%	100.0%						
Middle ($T = 4$)	GS+BNS ^{t_{max}}	8m	4.285	3.948	11.46%	8.3%	22m	5.058	3.965	15.29%	1.9%
	POMO-single	41s	4.281	3.855	11.50%	3.1%	2m	5.178	3.906	13.28%	1.1%
	AM	37s	4.329	3.857	10.53%	4.4%	2m	5.258	3.904	11.94%	1.8%
	POMO	8m	4.564	3.898	5.66%	9.1%	31m	5.645	3.932	5.46%	5.6%
	AM-MS	6m	4.566	3.895	5.65%	9.4%	30m	5.614	3.928	5.98%	6.3%
	AM-BS	6m	4.616	3.904	4.60%	16.1%	34m	5.711	3.939	4.35%	13.9%
	POMO+BNS ^{t_{max}}	12m	4.703	3.951	2.81%	29.6%	54m	5.840	3.959	2.26%	29.6%
	AM-BS+BNS ^{t_{max}}	13m	4.730	3.944	2.24%	39.0%	55m	5.846	3.962	2.09%	37.6%
	POMO+MNS ^{t_{max}} _[10,5]	31m	4.766	3.930	1.52%	43.1%	1.5h	5.882	3.947	1.49%	33.6%
	POMO+MNS _[10,10]	1.3h	4.839	3.940	0.00%	75.0%	3.7h	5.971	3.953	0.00%	65.5%
Wide ($T = 8$)	GS+BNS ^{t_{max}}	18m	8.062	7.954	11.19%	0.5%	1.1h	9.850	7.963	17.04%	0.1%
	POMO-single	1m	8.389	7.818	7.60%	1.1%	4m	10.875	7.889	8.41%	0.1%
	AM	1m	8.416	7.811	7.30%	0.7%	4m	10.829	7.884	8.79%	0.3%
	POMO	10m	8.747	7.860	3.69%	2.9%	1.2h	11.419	7.914	3.82%	0.8%
	AM-MS	12m	8.759	7.845	3.50%	6.0%	1.2h	11.341	7.913	4.48%	2.8%
	AM-BS	13m	8.766	7.866	3.43%	4.6%	1.2h	11.430	7.926	3.73%	2.1%
	POMO+BNS ^{t_{max}}	21m	8.935	7.955	1.49%	21.8%	2.2h	11.737	7.967	1.15%	23.4%
	AM-BS+BNS ^{t_{max}}	25m	8.979	7.947	1.09%	35.3%	2.2h	11.690	7.968	1.54%	28.4%
	POMO+MNS ^{t_{max}} _[10,5]	32m	8.989	7.920	0.98%	24.7%	2.4h	11.719	7.951	1.30%	12.4%
	POMO+MNS _[10,10]	3.0h	9.077	7.930	0.00%	53.3%	11.4h	11.873	7.954	0.00%	50.5%

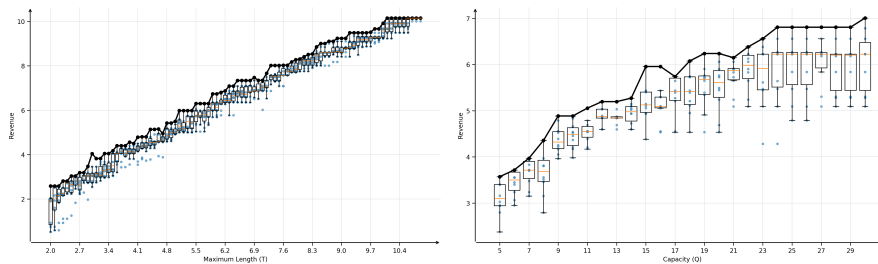
Notes: WR: Winning Rate. MSN: MSLNS, BNS: BI-LNS.

perience a performance drop when generalizing to larger instances (except for AM trained on PDSTSP82), which is expected due to the increased complexity and size of the problem. Models trained on PDSTSP42 suffer a pronounced drop when evaluated on PDSTSP82/122, whereas models trained on PDSTSP82 exhibit only minor degradation, indicating that both AM and POMO learn more scale-robust policies once exposed to mid-size instances. Note that this advantage is partly attributable to greater compute: PDSTSP82 models were trained for roughly $2\times$ the total time compared with PDSTSP42. Finally, POMO, AM-MS, and AM-BS effectively narrow the generalization gap by adapting candidates at test time.

We also assess POMO’s zero-shot ODD robustness to constraint tightness by varying T and Q to values not have been seen during training. As shown by Fig. 8, POMO maintains competitive performance across a wide range of T and Q ; since the best-achievable revenue should be monotone nondecreasing

Table 6: Performance matrix: PDSTSP82 vs. PDSTSP122 (Generalization from PDSTSP42) vs. PDSTSP122 (Generalization from PDSTSP82) on the *Distance* setting with Q and T randomly generated.

Algorithm	PDSTSP82 (42)				PDSTSP122 (42)				PDSTSP122 (82)			
	Time	Revenue	Profit	Gap	Time	Revenue	Profit	Gap	Time	Revenue	Profit	Gap
POMO-single	7m	9.54	2.55	14.29%	18m	13.92	3.23	22.80%	17m	16.51	6.00	8.43%
AM	6m	9.60	2.64	13.75%	18m	14.86	4.18	17.48%	13m	16.54	6.04	8.26%
AM-MS	1.1h	10.23	3.24	8.09%	2.9h	15.32	4.65	15.03%	2.4h	17.16	6.66	4.83%
AM-BS	1.1h	10.15	3.16	8.81%	2.9h	15.48	4.80	14.14%	2.9h	17.07	6.58	5.32%
POMO	1.1h	10.20	3.21	8.36%	2.9h	14.95	4.26	17.08%	2.0h	17.25	6.75	4.33%



(a) Zero-shot generalization across T ($Q = 10$) (b) Zero-shot generalization across Q ($T = 4$)

Figure 8: Out-of-distribution robustness to constraint tightness (the route-length budget T and vehicle capacity Q) of POMO on *Distance* PDSTSP42 with a randomly generated instance.

as constraints loosen, POMO’s curve closely tracks this trend with only minor deviations, indicating reliable adaptation to changing operating conditions without retraining. This robustness is crucial for real-world applications where constraints may vary frequently.

10.0.4 Different revenue settings

In this section, we evaluate each method under three revenue settings *Ton-Distance*, *Constant*, and *Uniform*—to study how payoff structure shapes routing behavior and relative performance. Across settings, we use the same instance generation, vehicle capacity Q , maximum route length T , and (when needed) normalize revenues to comparable scales. From Tab. 7, we observe that the relative performance of different algorithms remains consistent across revenue settings. This provides further support for the observations and conclusions drawn in the main text based on the distance setting. Hybrid methods that combine NCO with search (e.g., POMO+MSLNS and POMO+BI-LNS) consistently outperform pure NCO (e.g., POMO) and metaheuristics. POMO+MSLNS_[10,5]^{t_{max}} achieves near-optimal performance across all settings, but generally requires

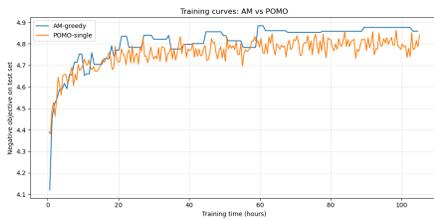
Table 7: Performance matrix: PDSTSP42 vs. PDSTSP82 across different revenue setting (*Ton-Distance/Constant/Uniform*) with Q and T randomly generated.

		PDSTSP42					PDSTSP82				
Algorithm		Time	Revenue	Profit	Gap	WR	Time	Revenue	Profit	Gap	WR
Ton-Distance	GS+BNS ^{t_{max}}	10m	16.224	12.275	10.81%	16.4%	1.2h	35.459	27.933	16.77%	2.5%
	GS+LNS ^{t_{max}}	17m	16.085	12.134	11.58%	16.9%	1.2h	35.897	28.372	15.74%	4.6%
	GS+SA ^{t_{max}}	20m	16.112	12.169	11.43%	25.7%	1.3h	34.541	27.022	18.93%	4.9%
	POMO-single	37s	16.060	12.207	11.72%	5.0%	4m	38.806	31.434	8.91%	1.1%
	POMO	6m	17.136	13.253	5.80%	15.7%	1.1h	40.725	33.328	4.41%	4.5%
	POMO+BNS ^{t_{max}}	15m	17.844	13.912	1.91%	49.2%	2.5h	41.979	34.520	1.47%	32.0%
	POMO+MNS ^{t_{max}} _[10,5]	30m	17.943	14.029	1.37%	54.7%	3.3h	42.084	34.674	1.22%	30.8%
	POMO+MNS _[10,10]	1.9h	18.191	14.271	0.00%	85.1%	16.4h	42.604	35.189	0.00%	81.0%
Uniform	GS+BNS ^{t_{max}}	13m	5.434	1.443	11.75%	12.4%	1.2h	11.165	3.960	16.91%	3.1%
	GS+LNS ^{t_{max}}	19m	5.342	1.346	13.24%	13.6%	1.3h	11.060	3.853	17.69%	2.5%
	GS+SA ^{t_{max}}	21m	5.395	1.407	12.38%	19.1%	1.5h	10.889	3.690	18.97%	3.9%
	POMO-single	46s	5.478	1.616	11.04%	5.6%	4m	12.207	5.158	9.15%	0.8%
	POMO	7m	5.840	1.934	5.16%	16.5%	1.3h	12.869	5.790	4.24%	4.0%
	POMO+BNS ^{t_{max}}	18m	6.054	2.078	1.68%	53.9%	2.8h	13.259	6.092	1.33%	37.1%
	POMO+MNS ^{t_{max}} _[10,5]	34m	6.083	2.135	1.20%	57.1%	3.6h	13.303	6.192	1.00%	36.7%
	POMO+MNS _[10,10]	2.2h	6.157	2.198	0.00%	86.1%	18.1h	13.438	6.323	0.00%	80.4%
Constant	GS+BNS ^{t_{max}}	11m	8.262	4.283	16.16%	19.9%	1.1h	16.798	9.772	22.07%	4.2%
	GS+LNS ^{t_{max}}	19m	8.168	4.192	17.12%	19.8%	1.4h	16.627	9.598	22.87%	4.1%
	GS+SA ^{t_{max}}	21m	8.571	4.584	13.03%	32.8%	1.5h	17.123	10.101	20.57%	7.1%
	POMO-single	47s	8.787	4.877	10.84%	26.4%	5m	19.729	12.825	8.48%	9.6%
	POMO	7m	9.418	5.482	4.43%	56.8%	1.5h	20.795	13.875	3.53%	33.8%
	POMO+BNS ^{t_{max}}	17m	9.643	5.730	2.15%	76.5%	2.7h	21.286	14.390	1.25%	72.7%
	POMO+MNS ^{t_{max}} _[10,5]	34m	9.786	5.855	0.70%	90.2%	3.9h	21.437	14.544	0.55%	85.8%
	POMO+MNS _[10,10]	2.3h	9.855	5.916	0.00%	97.0%	19.8h	21.556	14.653	0.00%	97.2%

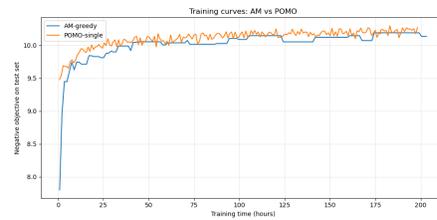
more time.

10.1 POMO vs. Attention Model

From the learning curves in Fig. 9, we see the same overall pattern on both sizes: most of the gain comes early (first 5-15 hours), after which improvements are smaller and the curves plateau. For PDSTSP42, the AM baseline climbs quickly and keeps a small but consistent edge over POMO-single near the end, whereas for PDSTSP82, the POMO-single continues to make small gains and slightly surpasses AM. POMO’s line is jaggier because we log every checkpoint; the AM line looks piecewise flat because we evaluate a fixed baseline that is not updated at every time point. Overall, AM is more competitive at the smaller scale, while POMO marginally overtakes as the problem size grows.



(a) AM v.s. POMO on PDSTSP42



(b) AM v.s. POMO on PDSTSP82

Figure 9: Learning curves for *Distance m1-PDSTSP* of REINFORCE with a greedy rollout baseline and POMO. After each training epoch, we generate 100 random instances and employ them as the test set.